

Resting state electroencephalographic alpha rhythms are sensitive to Alzheimer's disease mild cognitive impairment progression at a 6-month follow-up

Claudio Babiloni^{a,b,*}, Dharmendra Jakhar^{a,1}, Federico Tucci^a, Claudio Del Percio^a, Susanna Lopez^a, Andrea Soricelli^{c,d}, Marco Salvatore^c, Raffaele Ferri^e, Valentina Catania^e, Federico Massa^{f,g}, Dario Arnaldi^{f,h}, Francesco Famà^{f,h}, Bahar Güntekin^{i,j}, Görsev Yener^k, Fabrizio Stocchi^l, Laura Vacca^l, Moira Marizzoni^m, Franco Giubileiⁿ, Ebru Yıldırım^o, Lutfu Hanoğlu^p, Duygu Hünerli^q, Giovanni B. Frisoni^{m,r}, Giuseppe Noce^c

^a Department of Physiology and Pharmacology "Vittorio Erspamer", Sapienza University of Rome, Rome, Italy

^b Hospital San Raffaele Cassino, Cassino (FR), Italy

^c IRCCS Synlab SDN, Naples, Italy

^d Department of Medical, Movement and Wellbeing Sciences, University of Naples Parthenope, Naples, Italy

^e Oasi Research Institute - IRCCS, Troina, Italy

^f Dipartimento di Neuroscienze, Oftalmologia, Genetica, Riabilitazione e Scienze Materno-infantili (DiNOGMI), Università di Genova, Genova, Italy

^g Clinica neurologica, IRCCS Ospedale Policlinico San Martino, Genova, Italy

^h Neurofisiopatologia, IRCCS Ospedale Policlinico San Martino, Genova, Italy

ⁱ Department of Biophysics, School of Medicine, Istanbul Medipol University, Istanbul, Turkey

^j Research Institute for Health Sciences and Technologies (SABITA), Istanbul Medipol University, Istanbul, Turkey

^k Izmir University of Economics, Faculty of Medicine, Izmir, Turkey

^l IRCCS San Raffaele, Rome, Italy

^m Laboratory of Alzheimer's Neuroimaging and Epidemiology, IRCCS Istituto Centro San Giovanni di Dio Fatebenefratelli, Brescia, Italy

ⁿ Department of Neuroscience, Mental Health and Sensory Organs, Sapienza University of Rome, Rome, Italy

^o Program of Electroneurophysiology, Vocational School, Istanbul Medipol University, Istanbul, Turkey

^p Department of Neurology, School of Medicine, Istanbul Medipol University, Istanbul, Turkey

^q Health Sciences Institute, Department of Neurosciences, Dokuz Eylül University, Izmir, Turkey

^r Memory Clinic and LANVIE - Laboratory of Neuroimaging of Aging, University Hospitals and University of Geneva, Geneva, Switzerland

ARTICLE INFO

Keywords:

Resting state electroencephalographic (rsEEG) rhythms
Mild cognitive impairment due to Alzheimer's disease (ADMCI)
Alzheimer's disease progression
Exact Low-resolution Brain Electromagnetic Source Tomography (eLORETA)

ABSTRACT

Are posterior resting-state electroencephalographic (rsEEG) alpha rhythms sensitive to the Alzheimer's disease mild cognitive impairment (ADMCI) progression at a 6-month follow-up? Clinical, cerebrospinal, neuroimaging, and rsEEG datasets in 52 ADMCI and 60 Healthy old seniors (equivalent groups for demographic features) were available from an international archive (www.pdwaves.eu). The ADMCI patients were arbitrarily divided into two groups: REACTIVE and UNREACTIVE, based on the reduction (reactivity) in the posterior rsEEG alpha eLORETA source activities from the eyes-closed to eyes-open condition at $\geq -10\%$ and -10% , respectively. 75% of the ADMCI patients were REACTIVE. Compared to the UNREACTIVE group, the REACTIVE group showed (1) less abnormal posterior rsEEG source activity during the eyes-closed condition and (2) a decrease in that activity at the 6-month follow-up. These effects could not be explained by neuroimaging and neuropsychological biomarkers of AD. Such a biomarker might reflect abnormalities in cortical arousal in quiet wakefulness to be used for clinical studies in ADMCI patients using 6-month follow-ups.

* Correspondence to: Department of Physiology and Pharmacology "V. Erspamer", Sapienza University of Rome, P. le A. Moro 5, 00185 Rome, Italy.

E-mail address: claudio.babiloni@uniroma1.it (C. Babiloni).

¹ Equally contributing Authors

1. Introduction

Recent National Institute of Aging (NIA) and Alzheimer's Association (AA) guidelines posit that an AD diagnosis for research applications can be based on biomarkers derived from in-vivo measurement of amyloidosis ("A"), tauopathy ("T"), and neurodegeneration ("N") from the brain of patients living with AD, regardless their disease clinical manifestations (Jack et al., 2018). Those "A" and "T" biomarkers can be derived from cerebrospinal fluid (CSF) or positron emission tomography (PET) mapping. In contrast, "N" biomarkers can result from structural magnetic resonance imaging (sMRI) or fluorodeoxyglucose (FDG) PET mapping (Jack et al., 2018). This interesting neural model of AD is known as the **NIA-AA Framework** and is an important reference for field research.

In the NIA-AA Framework, there is no reference to how AD-related neuropathology and neurodegeneration may affect neurophysiological oscillatory mechanisms involving neuromodulatory subcortical ascending and cortical systems underpinning general cortical arousal and sleep-wake cycle (Hughes and Crunelli, 2005; Crunelli et al., 2015). Notably, these mechanisms promote the summation of action and post-synaptic potentials at cortical pyramidal neurons, producing detectable changes in the ongoing electromagnetic fields measured at the scalp level during wakefulness (Pfurtscheller and Lopes da Silva, 1999). These fields may be probed by the recording of ongoing scalp-recorded electroencephalographic (EEG) activity, which has a modest spatial resolution of some centimeters but a very high temporal resolution (milliseconds) to measure those rhythms spanning about 1–40 Hz during a resting state condition with eyes closed (Babiloni et al., 2020a; Babiloni et al., 2021b), namely the resting-state EEG (rsEEG) rhythms.

The rsEEG rhythms have been considered as candidate neurophysiological biomarkers to integrate the neural AD model of the NIA-AA Framework based on literature evidence (Babiloni et al., 2020a, 2020b, 2021a; Rossini et al., 2018, 2020). As compared to the control seniors with intact cognition (Healthy), AD patients with mild cognitive impairment (ADMCI) and dementia (ADD) were characterized by higher magnitude in rsEEG rhythms at delta (< 4 Hz) and theta (4–7 Hz) frequencies in widespread cortical regions as well as by lower magnitude in rsEEG rhythms at alpha (8–13 Hz) and beta (14–30 Hz) frequencies in central and posterior cortical regions; these effects were typically discussed as possibly due to the death of cortical neurons, axonal pathology, and cholinergic neurotransmission deficits (Babiloni et al., 2020, 2021; Rossini et al., 2020). Regarding cholinergic neurotransmission, posterior rsEEG alpha rhythms were lower in magnitude in ADMCI patients with greater than lower impairment in the cholinergic basal forebrain tract to the posterior cortex (Babiloni et al., 2009). Furthermore, posterior rsEEG alpha rhythms were lower in magnitude at 1-year follow-ups in ADD patients who did not clinically respond to the therapy with Acetylcholinesterase inhibitors (Babiloni et al., 2006).

The rsEEG rhythms have optimal features as candidate neurophysiological biomarkers of AD progression. In previous studies performed in healthy adults, they were found to be reproducible and reliable over time. It was shown that rsEEG power density spectra around the alpha frequencies were highly correlated (> 90%) between two rsEEG recordings performed with a retest interval of about 15 months (Näpflin et al., 2007). Similar correlations (> 90% for alpha bands) were observed between two rsEEG recordings performed with retest intervals of 25–62 months (Kondacs and Szabó, 1999). Furthermore, even broadband rsEEG power density measures were highly correlated with a retest interval from 5 min (> 90%) to about 1 month (> 80%) when 1 min of artifact-free EEG data was considered (Salinsky et al., 1991). Notably, slightly lower correlations (> 75% for alpha and beta bands) were reported in another study between two rsEEG recordings performed with retest intervals of 90 min and 1 month (Duan et al., 2021). The differences in the above findings may be mainly due to the different study procedures for the preliminary and spectral analysis of rsEEG data.

Several studies in AD patients have tested if rsEEG biomarkers can track the disease progression at 12 months or longer follow-ups. Compared to baseline recording sessions, ADD patients were characterized by a higher magnitude in rsEEG delta-theta rhythms (Soininen et al., 1989) at a follow-up of about 12 months, while ADMCI showed a lower magnitude in posterior rsEEG alpha rhythms at that follow-up (Babiloni et al., 2013). In another study, a group of ADMCI patients showed higher magnitude posterior rsEEG theta-delta rhythms and decreased rsEEG alpha-beta rhythms at a follow-up of 21 months (Jelic et al., 2000). Compared to MCI patients unaffected by AD, the ADMCI patients presented a higher magnitude in posterior rsEEG theta rhythms at a follow-up of 24 months (Jovicich et al., 2019). Furthermore, ADD patients were characterized by a higher magnitude in rsEEG delta-theta rhythms and a lower magnitude in rsEEG alpha rhythms at a follow-up of 24 months (Sloan and Fenton, 1993), while a higher magnitude in posterior rsEEG theta-delta rhythms and a lower magnitude in rsEEG alpha-beta rhythms were reported at a follow-up of 30 months (Coben et al., 1985).

The above results suggest that rsEEG alpha rhythms may reflect progressive abnormalities in the neurophysiological oscillatory mechanisms underpinning quiet wakefulness in ADD and ADMCI patients, although some variability in the spatial and frequency of the reported effects, especially at the dominant rsEEG alpha frequencies, motivated us to propose the following methodological approach (Babiloni et al., 2022). We arbitrarily qualified alpha rhythms as those having (1) a posterior maximum magnitude during the eyes-closed condition and (2) a significant reduction in that magnitude during the eyes-open condition according to the well-known phenomenon called **reactivity** or desynchronization of posterior rsEEG alpha rhythms, described for the first time by Hans Berger in 1929 (Berger, 1929; Gloor, 1994). Specifically, we arbitrarily defined a threshold for the rsEEG alpha-reactivity from the eyes-closed to open condition at equal or greater than –10%. Furthermore, we defined the bands of the alpha rhythms individually with the so-called **individual alpha frequency peak**, IAFp (Klimesch, 1999). In a reference study of our Consortium, this methodological approach showed a lower percentage of participants with substantial eyes-open reactivity in the posterior rsEEG alpha rhythms in the ADD patients (77%) than in the Healthy (93%) seniors (Babiloni et al., 2022).

The present study tested the hypothesis that in ADMCI patients showing a consistent magnitude of rsEEG alpha rhythms in the eyes-closed condition and a substantial reactivity in the transition to the eyes-open condition (arbitrarily defined as equal or greater than –10%; Babiloni et al., 2022), the posterior rsEEG alpha rhythms during the eyes-closed condition may be sensitive to the disease progression at the 6-month follow-up. Three groups of participants were considered: (1) the experimental group of ADMCI patients with rsEEG alpha reactivity during the eyes-open condition $\geq -10\%$; (2) the control group of ADMCI patients with rsEEG alpha reactivity during the eyes-open condition $< -10\%$; and (3) the control group of matched cognitively unimpaired (Healthy) participants. The two ADMCI groups received the rsEEG recordings at the baseline and the 6-month follow-up, while the Healthy group received only one rsEEG recording.

2. Materials and methods

2.1. Participants

We used the data from the PDWAVES Consortium archive (www.pdwaves.eu) to test this hypothesis. Specifically, we used clinical, neuropsychological, genetic, cerebrospinal fluid (CSF), magnetic resonance imaging (MRI), and rsEEG data collected from 52 ADMCI patients and 60 Healthy participants matched for age, sex, and education. They were previously recruited from the following clinical units: the Sapienza University of Rome (Italy), the University of Genoa (Italy), the Medipol University of Istanbul (Turkey), the Izmir University (Turkey), the

Institute for Research and Evidence-based Care (IRCCS) “Fatebenefratelli” of Brescia (Italy), the IRCCS SDN of Naples (Italy), the IRCCS Oasi Maria SS of Troina (Italy), and the IRCCS San Raffaele Pisana of Rome (Italy). All participants received (1) rsEEG recording in the conditions of eyes closed and open, (2) clinical and neuropsychological testing, and (3) structural MRIs at the baseline (T0) and a follow-up of 6 months (T6).

According to the NIA-AA guidelines, the diagnosis of AD was typically based on the positivity to the A β 1–42/phospho-tau ratio in the CSF considering the APOE ϵ 4 status (See [Supplementary Materials, 1. Cerebrospinal fluid A \$\beta\$ 42/P-tau cutoffs in patients with amnesic mild cognitive impairment](#)); in some cases, it was based on biomarkers of (1) brain hypometabolism, derived from 18 F-fluorodeoxyglucose positron emission tomography (FDG-PET), and (2) atrophy of the hippocampus, parietal, temporal, and posterior cingulate regions as revealed by volumetric MRIs ([Albert et al., 2011](#); [Jack et al., 2018](#)). That positivity was judged by the physicians in charge of releasing the clinical diagnosis to the patients, according to the local diagnostic routine of the participating clinical Units.

The clinical inclusion criteria for the selection of the ADMCI patients were as follows: (1) age of 55–90 years; (2) reported memory complaints confirmed by a relative; (3) Mini-Mental State Evaluation (MMSE) score of 24 or higher; (4) Clinical Dementia Rating (CDR) score of 0.5 ([Morris, 1993](#)); (5) logical memory test ([Wechsler, 1987](#)) score of 1.5 standard deviations (SD) lower than the mean adjusted for age; (2) the cognitive deficits had not to interfere significantly with the functional independence in the activities of daily living; (6) Geriatric Depression Scale (15-item GDS; [Brown and Schinka, 2005](#)) score of 5 or lower; (7) modified Hachinski ischemia ([Rosen et al., 1980](#)) score of 4 or lower; (8) education of 5 years or higher; and (8) amnesic syndrome within single or multi-domain MCI status.

The clinical exclusion criteria for the selection of the ADMCI patients were as follows: (1) other significant neurological, systemic, or psychiatric illness; (2) mixed dementing disease; (3) actual participation in a clinical trial using disease-modifying drugs; (4) systematic use of antidepressant drugs, including those with anticholinergic side effects; (5) chronic use of neuroleptics, narcotics, analgesics, sedatives or hypnotics (i.e., benzodiazepines); (6) anti-parkinsonian medications (cholinesterase inhibitors and Memantine allowed); (7) diagnosis of epilepsy or report of seizures or epileptiform EEG signatures in the past; and (8) major depression disorders described in the Diagnostic and Statistical Manual of Mental Disorders (DSM-5).

In all ADMCI patients, APOE4 genotyping and AD-relevant CSF biomarkers were assessed in a neurobiological definition of AD in line with the NIA-AA Research Framework ([Jack et al., 2018](#)). The CSF samples were preprocessed, frozen, and stored in line with the Alzheimer’s Association Quality Control Programme for CSF biomarkers ([Mattsson et al., 2011](#)). Dedicated single-parameter colorimetric enzyme-linked immunosorbent assay ELISA kits (Innogenetics, Ghent, Belgium) were used to measure amyloid beta 1–42 (i.e., A β 42). Levels of the protein tau (i.e., total tau, t-tau) and a phosphorylated form of tau at residue 181 (i.e., p-tau) were also measured. From one frozen aliquot of CSF, the assays were run parallel according to the manufacturer’s instructions. Each sample was assessed in duplicate. A standard sigmoidal curve was plotted to allow the quantitative expression (pg ml⁻¹) of measured light absorbance. All ADMCI patients in the present study were positive for the CSF A β 42/p-tau biomarker with a threshold defined in a previous investigation of our Workgroup ([Marizzoni et al., 2019](#)). In that investigation, the positivity cut-off to that CSF A β 42/p-tau biomarker was 15.2 for APOE4 carriers and 8.9 for APOE4 non-carriers. In the present study, all ADMCI patients with APOE4 status had the CSF A β 42/p-tau lower than 15.2, whereas the ADMCI patients without APOE4 status had the CSF A β 42/p-tau lower than 8.9.

Furthermore, in all ADMCI patients, relevant MRI markers were measured at baseline and 6-month follow-up. All MRI scans were performed using 3.0 Tesla machines. The MRI protocol consisted of several

acquisitions, including two anatomical T1, anatomical T2, fluid-attenuated inversion recovery (FLAIR), and diffusion tensor imaging scans. Only anatomical T1 scans were available for all units and were analyzed in the present study. The centralized MRI analysis visually inspected all data for quality assurance before extracting the MRI biomarkers. Specifically, we checked that there were no gross partial brain coverage errors or major visible artifacts, including motion, wrap-around, radio frequency interference, and signal intensity or contrast inhomogeneities. The two anatomical T1 scans were averaged, and the anatomical scans obtained were analyzed using FreeSurfer version 5.1.0 to automatically generate (1) MRI-based volumes of the hippocampus and lateral ventricle (normalized with respect to the total intracranial volume, TIV) for the left and right hemispheres and (2) MRI-based cortical thicknesses of the parahippocampal gyrus, fusiform gyrus, entorhinal cortex, precuneus, and cuneus for the left and right hemispheres.

In all ADMCI patients, global cognitive status and performances in various cognitive domains (e.g., episodic memory, language, executive function, attention, and visuospatial function) were assessed at the baseline and the 6-month follow-up. Specifically, (1) global cognitive status was tested by MMSE and Alzheimer’s Disease Assessment Scale–Cognitive Subscale (ADAS-Cog; [Folstein et al., 1975](#); [Rosen et al., 1984](#)); (2) episodic memory was assessed by immediate and delayed recall of Rey Auditory Verbal Learning Test ([Rey, 1968](#)); (3) language function was evaluated by 1-min Verbal fluency test for letters ([Novelli et al., 1986](#)) and 1-min Verbal fluency test for category (fruits, animals or car trades; [Novelli et al., 1986](#)); (4) executive functions and attention were tested by Trail making test (TMT) parts A and B ([Reitan, 1958](#)); and (5) visuospatial functions were assessed by Clock drawing test ([Freedman et al., 1994](#)).

The use of selective serotonin reuptake inhibitors (SSRIs), noradrenaline reuptake inhibitors (SNRIs), acetylcholinesterase inhibitors (AChEIs), and inhibitors of N-methyl-D-aspartate receptors (iNMDARs) were allowed in all ADMCI patients. The ADMCI patients using those drugs could take their medications immediately after the rsEEG experiments, which were planned in the late morning. Therefore, the ADMCI patients delayed the intake of their medications only for a few hours during their routine.

All Healthy seniors underwent a cognitive screening (including MMSE and GDS) and physical and neurological examinations to exclude subjective memory complaints (SMCs), cognitive deficits, and mood disorders. They had an MMSE score equal to or greater than 27, a CDR score equal to 0, and a GDS score lower than the threshold of 5 (no depression) or were evaluated as having no depression after an interview with a physician or a clinical psychologist at the time of the enrolment. The Healthy seniors with previous or present neurological or psychiatric disease were excluded. Furthermore, the Healthy seniors affected by any chronic systemic illnesses (e.g., diabetes mellitus) were excluded, as were the Healthy seniors taking chronically psychoactive drugs. Unfortunately, the Healthy datasets were not available at the 6-month follow-up.

[Table 1](#) summarizes the most relevant demographic (i.e., age, sex, and education attainment) and clinical (i.e., MMSE score) features observed in the Healthy (N = 60) and ADMCI (N = 52) groups. Furthermore, [Table 1](#) reports the results of the presence or absence of statistically significant differences (p < 0.05) between the two groups for age (T-test), sex (Fisher test), educational attainment (T-test), and MMSE score (Mann Whitney U test). As expected, a statistically significant difference was found in the MMSE score (p < 0.00001), showing a higher score in the Healthy than the ADMCI group. On the contrary, no statistically significant differences were found in the age, sex, and educational attainment between the groups (p > 0.05).

[Table 2](#) reports the most relevant clinical (i.e., GDS, CDR, and Hachinski Ischemic Score), genetic (i.e., APOE genotyping), and CSF (i.e., A β 42, t-tau, p-tau, and A β 42/p-tau) features in the ADMCI group (N = 52). [Table 2](#) also reports the number and the percentages of ADMCI

Table 1
Demographic and clinical data in healthy and ADMCI.

	Healthy	ADMCI	Statistical analysis
N	60	52	-
Age (years, mean \pm SE)	69.1 \pm 0.9	69.6 \pm 0.9	T-test = n.s.
Sex (M/F)	28/32	20/32	Fisher test = n.s.
Education (years, mean \pm SE)	11.0 \pm 0.6	11.3 \pm 0.6	T-test = n.s.
MMSE (scores, mean \pm SE)	28.6 \pm 0.2	26.5 \pm 0.3	Mann-Whitney U test: p < 0.00001

Table 1. Mean values (\pm standard error of the mean, SE) of the demographic and clinical data as well as the results of their statistical comparisons ($p < 0.05$) in the groups of cognitively normal older adults (Healthy, N = 60) and patients with mild cognitive impairment due to Alzheimer's disease (ADMCI, N = 52). Legend: M/F = males/females; n.s. = not significant ($p > 0.05$); MMSE = Mini-Mental State Evaluation.

Table 2
Clinical, genetic (APOE), cerebrospinal fluid markers, and drugs in the ADMCI group.

Clinical markers	
Geriatric depression scale (GDS)	2.6 \pm 0.2
Clinical dementia rating (CDR)	0.5 \pm 0.0
Hachinski ischemic score (HIS)	0.8 \pm 0.1
Genetic marker	
APOE4 (%)	81%
Cerebrospinal fluid markers	
A β 42 (pg/ml)	502 \pm 20
p-tau (pg/ml)	84 \pm 5
t-tau (pg/ml)	592 \pm 44
A β 42/p-tau	7.0 \pm 0.4
Drugs	
Selective serotonin reuptake inhibitors (SSRIs; N, %)	25% (N = 13)
Selective serotonin and noradrenaline reuptake inhibitors (SNRIs, N, %)	7.7% (N = 4)
Acetylcholinesterase inhibitors (AChEIs; N, %)	15.4% (N = 8)
Antagonists of N-methyl-D-aspartate receptors (aNMDARs, N, %)	0% (N = 0)

Table 2. Mean values (\pm SE) of the clinical (i.e., Geriatric Depression Scale, Clinical Dementia Rating, and Hachinski Ischemic Score), genetic (i.e., Apolipoprotein E genotyping, APOE), and cerebrospinal fluid (i.e., beta-amyloid 1-42, A β 42; protein tau, t-tau; a phosphorylated form of the protein tau, p-tau; and A β 42/ p-tau ratio) data in the ADMCI patients (N = 52). In line with the inclusion criteria, all ADMCI patients had a CDR score of 0.5, a GDS score of ≤ 5 , and an HIS score of ≤ 4 . The number and percentages of ADMCI patients assuming the selective serotonin reuptake inhibitors (SSRIs), selective serotonin and noradrenaline reuptake inhibitors (SNRIs), acetylcholinesterase inhibitors (AChEIs), and antagonists of N-methyl-D-aspartate receptors (aNMDARs) are also reported.

patients assuming the following drug classes: selective serotonin reuptake inhibitors (SSRIs), noradrenaline reuptake inhibitors (SNRIs), acetylcholinesterase inhibitors (AChEIs), and inhibitors of N-methyl-D-aspartate receptors (iNMDARs).

The local institutional Ethical Committees approved the study. All experiments were performed with each participant or caregiver's informed and overt consent, in line with the Code of Ethics of the World Medical Association (Declaration of Helsinki) and the standards established by the local Institutional Review Board.

2.2. The rsEEG recordings

The electrophysiological data were recorded by professional digital EEG systems licensed for clinical applications. The following digital EEG systems were used: BrainAmp 32-Channel DC System (Brain Product GmbH, Germany), Waveguard caps (ANT Neuro, The Netherlands), EB Neuro-BE LIGHT (EB Neuro, Italy), Galileo NT Line - EB Neuro (EB Neuro, Italy), and EB Neuro- Sirius BB (EB Neuro, Italy).

As mentioned above, the rsEEG recordings were performed at the baseline and the 6-month follow-up in the ADMCI patients and just at the baseline in the Healthy seniors.

All rsEEG recordings were performed in the late morning. The rsEEG recordings were performed in all participants using at least 19 scalp exploring electrodes, placed according to the 10–20 system. The selected electrode location is illustrated in the [Supplementary Materials](#) (see Figure SM1).

The ground electrode was attached to the right clavicle or on the forehead, while linked earlobes (A1 and A2) or Fpz were the active reference for all the electrodes during recording. Electrode impedance was maintained below 5 k Ω ; continuous EEG data were recorded at 128–1024 Hz sampling frequency and related antialiasing bandpass between 0.01 Hz and 60–100 Hz. Horizontal and vertical electrooculographic (EOG) potentials (0.3–70 Hz bandpass) were also recorded to control eye movements and blinking.

The participants were seated in a comfortable armchair during the rsEEG recording and instructed to remain awake, psychophysically relaxed (no movement), and with the mind freely wandering (no mental planning or cognitive operations). Based on the instructions given by an experimenter, each rsEEG recording lasted 3–5 min in the condition of eyes closed, followed by 3–5 min in the condition of eyes open. The experimenter supervised participants during the rsEEG recording to monitor adherence to the protocol. The experimenter instructed participants to adhere to the protocol if needed. All deviations by the protocol and verbal interventions were annotated and used during the phase of rsEEG data analysis.

2.3. Preliminary rsEEG data analysis

The rsEEG data were centrally analyzed by experts blinded to the participants' diagnosis by the Sapienza University of Rome unit. The recorded rsEEG data were exported as a European data format (.edf) file and then processed offline using the EEGLAB toolbox (Delorme and Makeig, 2004; version eeglab14_1_2b) running in the MATLAB software (Mathworks, Natick, MA, USA; version: R2014b). The rsEEG data were divided into epochs lasting 2 s (i.e., 5 min = 150 rsEEG epochs of 2 s for each experimental condition) and analyzed offline.

Afterward, the EEG datasets were analyzed by a 3-step procedure aimed at detecting and removing (1) recording channels (electrodes) showing prolonged artefactual rsEEG activity due to bad electric contacts or other reasons, (2) rsEEG epochs with artifacts at recording channels characterized by general good signals, and (3) intrinsic components of the rsEEG epochs with artifacts.

The first step was based on a visual analysis of the recorded rsEEG activity by two independent experimenters among six experts (i.e., C.D.P, G.N., S.L., F.T., and D.J.) for a first identification of the selected electrodes affected by irremediable artifacts. Indeed, no more than 3 selected electrodes were removed for each participant. For the clinical units with a digital EEG system using > 19 exploring electrodes, the removed electrodes were substituted with the nearest electrodes not included among the 19 selected electrodes. The added electrodes were then used together with the artifact-free selected electrodes to compute the interpolation of artifact-free rsEEG data at all scalp sites of the removed electrodes (EEGLAB toolbox, Delorme A and Makeig S, 2004; version eeglab14_1_2b), thus ensuring that all participants had artifact-free EEG data at the locations of the 19 selected electrodes.

The second step was based on a visual analysis of the recorded rsEEG activity by two of the mentioned independent experimenters (i.e., C.D.P, G.N., S.L., F.T., and D.J.) for the first selection of artefactual rsEEG epochs. The rsEEG epochs contaminated by muscular, ocular, head movements, or non-physiological artifacts were removed.

The third step was implemented by an independent component analysis (ICA) from the EEGLAB toolbox, applied to remove the ICA components representing the residual artifacts due to (1) blinking and eye movements, (2) involuntary head movements, (3) neck and shoulder

muscle tensions, and (4) electrocardiographic activity (Crespo-Garcia et al., 2008; Jung et al., 2000). For each rsEEG dataset, fewer than five ICA components were removed from the original ICA solutions based on 19 ICA components. In the third step, the rsEEG datasets were reconstructed with the remaining (artifact-free) ICA components. The putative artifact-free rsEEG epochs were visually double-checked again by two of the mentioned independent experimenters (i.e., C.D.P., G.N., S.L., F.T., and D.J.) to confirm or make the final decision about the inclusion or the exclusion of each of those rsEEG epochs.

The artifact-free EEG data for the common 19 electrodes were used as input for two additional methodological steps. The first additional step served to harmonize rsEEG data recorded by the clinical units using different reference electrodes and sampling frequency rates. The rsEEG data were frequency-band passed at 0.5–45 Hz and down-sampled, when appropriate, to make the sampling rate of all artifact-free rsEEG datasets in the Healthy and ADMCI participants equal to 128 Hz. Furthermore, all those rsEEG epochs were re-referenced to the common average reference.

The second additional step minimizes the habituation effects in the rsEEG data recorded during the eyes-open condition. Only the first minute of those rsEEG data (when the rsEEG alpha reactivity is supposed to be well-represented) was considered in the further analyses.

As a result of the above procedures, the artifact-free epochs showed a similar proportion (> 75%) of the total amount of rsEEG activity recorded in the two groups of participants (i.e., Healthy and ADMCI) and all rsEEG recordings (baseline and 6-month follow-up for the ADMCI participants).

2.4. Spectral analysis of the rsEEG epochs

A standard digital FFT-based analysis (Welch technique, Hanning windowing function, no phase shift) computed the power density of artifact-free rsEEG epochs at all 19 scalp electrodes (0.5 Hz of frequency resolution). From those spectral solutions, the rsEEG frequency bands of interest were individually identified based on the following frequency landmarks: the transition frequency (TF) and the alpha-background frequency (BGF) observed in the eyes-closed condition. In the eyes-closed rsEEG power density spectrum, the TF was defined as the minimum rsEEG power density between 3 and 8 Hz, while the individual alpha-BGF peak was defined as the maximum power density peak between 6 and 14 Hz. As mentioned in the Introduction, that frequency is also called IAFp (Klimesch, 1999). The TF and alpha-BGF were computed for each participant involved in the study. Based on the TF and alpha-BGF, we estimated the individual delta, theta, and alpha-BGF bands as follows: delta from $TF - 4$ Hz to $TF - 2$ Hz, theta from $TF - 2$ Hz to TF, low alpha-BGF (BGF 1 and BGF 2) from TF to alpha-BGF peak, and high-frequency alpha-BGF (or BGF 3) from alpha-BGF to $BGF + 2$ Hz. Specifically, the individual alpha-BGF 1 and alpha-BGF 2 bands were computed as follows: BGF 1 from TF to the frequency midpoint of the TF-BGF range and BGF 2 from that midpoint to the BGF peak. Suppose IAFp is observed at 9 Hz in a given participant. In that case, the individual alpha 1 sub-band typically ranges from 5 to 7 Hz, the individual alpha 2 sub-band from 7 to 9 Hz, and the individual alpha 3 sub-band from 9 Hz to 11 Hz. Notably, Dr. Klimesch's work showed that these individual alpha sub-bands are differently associated with (de)synchronization of EEG alpha rhythms related to general vigilance (arousal) level, attention, and memory functions (Klimesch, 1997, 1999; Vogt et al., 1998). Notably, in the present study, the BGFs were arbitrarily denoted as “alpha rhythms” if there was a substantial reduction in magnitude (reactivity) of the rsEEG rhythms at the alpha range from the eyes-closed to the eyes-open condition, as explained in another section of this chapter on the methodology.

The other bands were defined based on the standard fixed frequency ranges used in the reference rsEEG studies of our Consortium (Babiloni et al., 2017a, 2017b, 2019, 2020b): beta 1 from 14 to 20 Hz, beta 2 from 20 to 30 Hz, and gamma from 30 to 40 Hz.

Figure 1 illustrates an example of the global scalp normalized eyes-closed rsEEG power density spectrum with frequency bands definition.

2.5. Cortical sources of rsEEG epochs as computed by eLORETA

Previous reference articles of our Consortium described the procedures for the rsEEG cortical source estimations (Babiloni et al., 2017a, 2017b, 2019, 2020b). We used the official freeware tool called eLORETA (eLORETA) to linearly estimate the cortical source activity generating scalp-recorded rsEEG rhythms (Pascual-Marqui, 2007). The present implementation of the eLORETA freeware uses a head volume conductor model composed of the scalp, skull, and brain. In the scalp compartment, the exploring electrodes can be virtually positioned to give EEG data as an input to the source estimation (Pascual-Marqui, 2007). The brain model is based on a realistic cerebral shape from a template typically used in neuroimaging studies, namely that of the Montreal Neurological Institute (MNI152 template). The eLORETA freeware solves the so-called EEG inverse problem from scalp-recorded EEG activity, estimating the associated “neural” current density values at any cortical voxel of the mentioned head volume conductor model. The cortical source solutions are computed at each voxel of the brain model and each frequency bin.

For the estimation of EEG cortical source activities (i.e., the eLORETA solutions), the input is the EEG spectral power density computed at the 19 scalp electrodes. This estimation is performed in the electrical brain source space formed by 6239 voxels with 5 mm resolution, restricted to the cortical grey matter of the head volume conductor model. Into each voxel, an equivalent current dipole is located to represent the mean ionic currents generated by the local populations of cortical pyramidal neurons. The eLORETA package provides the Talairach coordinates, the lobe, and the Brodmann area (BA) for each voxel of the brain model.

The eLORETA solutions from the rsEEG data were normalized by the following procedure. We averaged the eLORETA solutions across (1) the two experimental conditions (i.e., resting-state eyes-closed and eyes-open conditions), (2) all frequency bins from 0.5 to 45 Hz, and (3) 6239 voxels of the brain model volume to obtain the eLORETA “mean” solution. Afterward, we computed the ratio between any original eLORETA solution at a given condition/frequency-bin/voxel and the eLORETA mean solution. As a result, any original eLORETA solution at a given condition/frequency-bin/voxel changed to a normalized eLORETA solution.

In line with the general low spatial resolution of the current EEG methodological approach (i.e., 19 scalp electrodes), we performed a regional analysis of the eLORETA solutions. For this purpose, we separately collapsed the eLORETA solutions within frontal, central, parietal, occipital, temporal, and limbic macro-regions (ROIs). The BAs used for the ROIs considered in the present study can be found in the [supplementary materials](#). (Table SM01).

For the present eLORETA cortical source estimation, a frequency resolution of 0.5 Hz was used, namely, the maximum frequency resolution allowed using 2-s artifact-free EEG epochs.

2.6. The computation of the rsEEG alpha-background frequency (BGF) reactivity

To analyze the rsEEG alpha-BGF reactivity from the eyes-closed to the eyes-open condition, we considered the eLORETA source solutions estimated in the central, parietal, and occipital ROIs. Based on the reference rsEEG studies of our Consortium (Babiloni et al., 2017a, 2017b, 2019, 2020b), the rsEEG alpha-BGF reactivity was measured at the alpha-BGF 2 frequency band, which showed the maximum source activities in the Healthy participants during the eyes-closed condition.

The reactivity-dependent variable for the statistical analyses was obtained by averaging the eLORETA alpha-BGF 2 source solutions in the central, parietal, and occipital ROIs. To avoid habituation effects in the

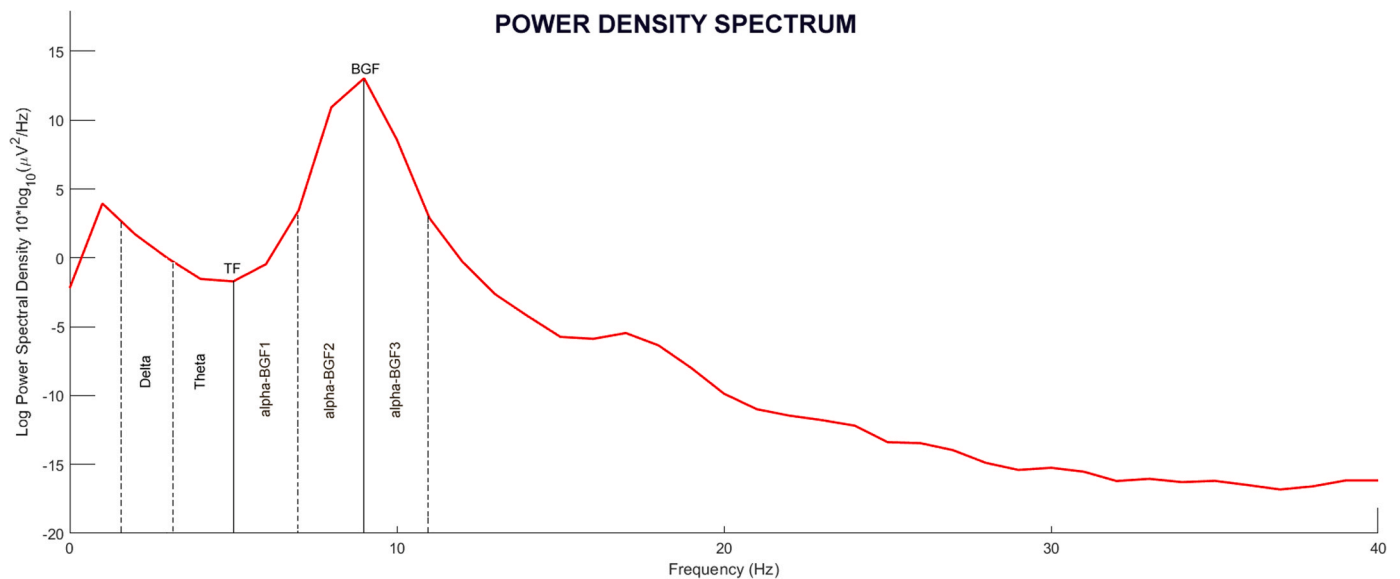


Fig. 1. Example of global scalp normalized power density spectrum from eyes-closed resting-state electroencephalographic (rsEEG) rhythms in humans. For each frequency bin (0.5–45 Hz), such a spectrum was calculated by averaging the normalized scalp rsEEG power density values across all 19 electrodes of a 10–20 montage system. The rsEEG frequency bands of interest were individually identified based on the following frequency landmarks: transition frequency (TF) and alpha-background frequency (BGF) peak. According to Dr. W. Klimesch (1999), the alpha-BGF peak is also called the individual alpha frequency peak (IAFp). The low-frequency alpha-BGF sub-bands, such as alpha 1 (BGF 1) and alpha 2 (BGF 2), range from the TF to the alpha-BGF peak (IAFp). Furthermore, the high-frequency alpha sub-band, alpha 3 (e.g., BGF 3), ranges from the alpha-BGF peak to + 2 Hz. The delta and theta parts of the rsEEG power density spectrum denote the frequency bands at lower frequencies with respect to the alpha (BGF) bands. In healthy adults, the rsEEG rhythms from the eyes-closed condition show a dominant, ample power density peak at the alpha (BGF) band at parietal and occipital scalp electrodes. Furthermore, this peak significantly reduces its power density during the eyes-open resting-state condition (not shown).

eyes-open condition, that reactivity was computed based on the eLOR-ETA solutions estimated during the first minute of the rsEEG recordings (when the rsEEG alpha-BGF reactivity is maximum). As no significant habituation effect was described in the eyes-closed condition, eLORETA solutions were estimated during all five minutes of the rsEEG recordings in that condition.

The rsEEG alpha-BGF reactivity from the eyes-closed to the eyes-open condition was computed by the following formula:

$$\text{Reactivity}(\%) = \frac{\text{eyes open} - \text{eyes closed}}{\text{eyes closed}} * 100$$

According to this definition, the percent negative values (i.e., weaker alpha-BGF source activities during the eyes-open than the eyes-closed condition) indexed a reduction (reactivity) in the source alpha-BGF activities from the eyes-closed to the eyes-open condition (Babiloni et al., 2010; Del Percio et al., 2011). On the contrary, the percent positive values (i.e., greater BGF source activities during the eyes-open than the eyes-closed condition) indexed an increase in the source alpha-BGF activities from the eyes-closed to the eyes-open condition.

The individual values of the reactivity (%) of the central-parietal-occipital rsEEG (eLORETA) alpha-BGF 2 source activity from the eyes-open (1 min) to the eyes-closed (5 min) condition for all Healthy (N = 60) and ADMCI (N = 52) participants are illustrated in [Supplementary Materials \(4. Details on individual rsEEG data analysis and the statistical results of rsEEG source solutions; Figure SM2\)](#). For the ADMCI participants, those individual values are plotted for the rsEEG recordings at baseline and 6-month follow-up.

In the present study, we applied an arbitrary threshold for the alpha-BGF source reactivity of – 10% (Babiloni et al., 2022). Based on this threshold, we identified 5 Healthy participants and 13 ADMCI patients who did not exhibit significant BGF reactivity at the baseline, such reactivity defined above. Thus, the BGF-2 source reactivity was detected in 55 out of 60 Healthy seniors and 39 out of 52 ADMCI patients at the baseline. In the following analyses, we will refer to them as alpha-reactive participants. Moreover, the BGF-2 source reactivity was

detected in 32 out of 39 alpha-reactive ADMCI patients at the 6-month follow-up. In the following analyses, we will refer to them as 6-month follow-up alpha-reactive participants. Table SM2 of the [Supplementary Materials](#) illustrates the relevant demographic (i.e., age, sex, and education attainment) and clinical (i.e., MMSE score) features in the subgroups of the alpha-reactive Healthy seniors (N = 55) and alpha-reactive ADMCI patients (N = 39). Furthermore, this table reports the results of the presence or absence of statistically significant differences ($p < 0.05$) between the two subgroups for age (T-test), sex (Fisher test), educational attainment (T-test), and MMSE score (Mann Whitney U test). As expected, a statistically significant difference was found for the MMSE score ($p < 0.00001$), showing a higher score in the alpha-reactive Healthy than the alpha-reactive ADMCI subgroup. On the contrary, no statistically significant differences were found in age, sex, and educational attainment between the subgroups ($p > 0.05$; see also [Supplementary Materials, 4. Details on individual rsEEG data analysis and the statistical results of rsEEG source solutions; Table SM02](#)).

The subgroups of alpha-reactive ADMCI participants (N = 39) clinical (i.e., GDS, CDR, and Hachinski Ischemic Score), genetic (i.e., *APOE* genotyping), and CSF (i.e., A β 42, t-tau, p-tau, and A β 42/ p-tau) and percentages of the ADMCI patients assuming the following drug classes: selective serotonin reuptake inhibitors (SSRIs), noradrenaline reuptake inhibitors (SNRIs), acetylcholinesterase inhibitors (AChEIs), and inhibitors of N-methyl-D-aspartate receptors (iNMDARs) is reported; see [Supplementary materials Table SM03](#).

The relevant demographic (age, sex, educational attainment) clinical (i.e., GDS, CDR, and Hachinski Ischemic Score), genetic (i.e., *APOE* genotyping), CSF (i.e., A β 42, t-tau, p-tau, and A β 42/ p-tau), and the percentages of the ADMCI patients assuming the drug classes mentioned above for the subgroups of 6-month follow-up alpha-reactive ADMCI patients (N = 32) is also reported; see [Supplementary materials Table SM04](#).

2.7. Statistical analysis of the rsEEG source activity

Three statistical sessions were performed by the commercial tool STATISTICA 10 (StatSoft Inc., www.statsoft.com) to test the control hypothesis and the two working hypotheses. In all the statistical sessions, an ANOVA was computed using the eyes-closed rsEEG source activities (i.e., regional normalized eLORETA solutions) as a dependent variable ($p < 0.05$). Mauchly's test evaluated the sphericity assumption, and degrees of freedom were corrected by the Greenhouse-Geisser procedure when appropriate ($p < 0.05$). Duncan test was used for posthoc comparisons using a statistical threshold of $p < 0.05$ Bonferroni corrected for the planned contrasts.

It is well-known that the use of ANOVA models implies that dependent variables approximate Gaussian distributions, so we tested this feature in the regional normalized eLORETA current densities of interest by the Kolmogorov-Smirnov test. The hypothesis of Gaussian distributions was tested at $p > 0.05$ (i.e., $p > 0.05 = \text{Gaussian}$, $p \leq 0.05 = \text{non-Gaussian}$). As the distributions of the regional normalized eLORETA current densities were not Gaussian in several cases, all eLORETA variables underwent the $\log_{10}(x + 1)$ transformation (\log_{10} transformed) and re-tested ($p > 0.05 = \text{Gaussian}$). Such a transformation is a popular method to transform skewed data distribution with all positive values (as regional normalized eLORETA current densities are) to Gaussian distributions, thus augmenting the reliability of the ANOVA results. Indeed, the outcome of the procedure approximated the distributions of all regional normalized eLORETA current densities to Gaussian distributions ($p > 0.05 = \text{Gaussian}$), allowing the use of the ANOVA model.

The results of the following statistical analyses were controlled by the iterative (leave-one-out) Grubbs' test detecting for the presence of one or more outliers in the distribution of the eLORETA source solutions. The null hypothesis of the non-outlier status was tested at the arbitrary threshold of $p < 0.01$ to remove only individual values with a high probability of being outliers.

The first ANOVA tested the control hypothesis that the eyes-closed rsEEG source activities (i.e., regional normalized eLORETA solutions) were abnormal in the ADMCI group ($N = 52$) as compared to the Healthy group ($N = 60$). The ANOVA factors were Group (Healthy and ADMCI), Band (delta, theta, BGF1, BGF2, BGF3, beta 1, beta 2, and gamma), and ROI (frontal, central, parietal, occipital, temporal, and limbic). The confirmation of the control hypothesis may require the following results: (1) a statistically significant ANOVA effect including the factor Group ($p < 0.05$) and (2) a post-hoc Duncan test indicating statistically significant ($p < 0.05$ Bonferroni corrected) differences in the eyes-closed rsEEG source activities between the Healthy and ADMCI groups (i.e., Healthy \neq ADMCI, $p < 0.05$ Bonferroni corrected).

The second ANOVA evaluated the first working hypothesis that the eyes-closed rsEEG source activities (i.e., regional normalized eLORETA solutions) were abnormal in the alpha-reactive ADMCI group ($N = 39$) as compared to the alpha-reactive Healthy group ($N = 55$). The ANOVA factors were Group (alpha-reactive Healthy and alpha-reactive ADMCI), Band (delta, theta, alpha 1, alpha 2, alpha 3, beta 1, beta 2, and gamma), and ROI (frontal, central, parietal, occipital, temporal, and limbic). The confirmation of the control hypothesis may require: (1) a statistically significant ANOVA effect including the factor Group ($p < 0.05$) and (2) a post-hoc Duncan test indicating statistically significant ($p < 0.05$ Bonferroni corrected) differences in the eyes-closed rsEEG source activities between the alpha-reactive Healthy group and the alpha-reactive ADMCI group (i.e., alpha-reactive Healthy \neq alpha-reactive ADMCI, $p < 0.05$ Bonferroni corrected).

The third ANOVA evaluated the second working hypothesis that the eyes-closed rsEEG source activities (i.e., regional normalized eLORETA solutions) deteriorated across time (6 months) in the 6-month follow-up alpha-reactive ADMCI group ($N = 32$). The ANOVA factors were Time (baseline and 6-month follow-up), Band (delta, theta, alpha 1, alpha 2, alpha 3, beta 1, beta 2, and gamma), and ROI (frontal, central, parietal, occipital, temporal, and limbic). The confirmation of this second

working hypothesis may require: (1) a statistically significant ANOVA effect including the factor Time ($p < 0.05$) and (2) a post-hoc Duncan test indicating statistically significant ($p < 0.05$ Bonferroni corrected) differences in the rsEEG source activities between the baseline and 6-month follow-up in the 6-month follow-up alpha-reactive ADMCI participants (i.e., baseline \neq follow-up, $p < 0.05$ Bonferroni corrected). We further evaluate the effect size of the statistically significant post-hoc comparisons by means of Cohen's d (statistical power of 0.8).

3. Results

3.1. Individual frequencies and distributions of rsEEG source activities in the Healthy and ADMCI groups

The mean TF was 5.7 Hz (± 0.1 SE) in the Healthy group ($N = 60$) and 5.2 Hz (± 0.2 SE) in the ADMCI group ($N = 52$). Furthermore, the mean BGF was 9.1 Hz (± 0.1 SE) in the Healthy group and 8.9 Hz (± 0.2 SE) in the ADMCI group. The T-tests of these data showed that the mean TF was greater in the Healthy than in the ADMCI group ($p < 0.005$). No statistically significant difference was found for the mean BGF ($p > 0.05$).

The results of the first statistical session about the eyes-closed rsEEG source activities in all participants are illustrated in Figure 2. It shows the mean values (\pm SE, \log_{10} transformed) of the regional rsEEG (eLORETA) source activities during the eyes-closed condition in the Healthy ($N = 60$) and ADMCI ($N = 52$) groups. The distribution of those source activities differed across the groups, the ROIs, and the bands. In the Healthy group, as a physiological reference, the temporal, parietal, and occipital (eLORETA) alpha-BGF2 and alpha-BGF3 source activities showed dominant values among all ROIs. Relatively low values in all ROIs characterized delta, theta, and alpha-BGF1 source activities, while the beta and gamma source activities were generally very low. Compared to the Healthy group, posterior rsEEG alpha-BGF2, and alpha-BGF3 source activities were substantially lower in the ADMCI group. Furthermore, the ADMCI group exhibited increased widespread delta and theta source activities.

Based on these input data, the ANOVA results showed a statistical interaction effect ($F(35, 3850) = 3.67$, $p < 0.00001$) among the factors Group (Healthy and ADMCI), Band (delta, theta, alpha-BGF1, alpha-BGF2, and alpha-BGF3, beta 1, beta 2, and gamma), and ROI (frontal, central, parietal, occipital, temporal, and limbic). The Duncan planned post-hoc ($p < 0.05$ Bonferroni correction for 8 Bands \times 6 ROIs, $p < 0.05/48 = 0.001$) testing produced the following core results: (1) the discriminant pattern Healthy $<$ ADMCI was fitted by the frontal, central, parietal, occipital, and temporal delta source activities ($p < 0.00005 - 0.000005$) as well as the frontal, parietal, occipital, and temporal theta source activities ($p < 0.0001 - 0.000005$); and (2) the discriminant pattern Healthy $>$ ADMCI was fitted by the central, parietal occipital, temporal, and limbic alpha-BGF2 source activities ($p < 0.0005 - 0.000005$) as well as the central, parietal, occipital, temporal, and limbic alpha-BGF3 source activities ($p < 0.00005 - 0.000001$). The size effects of these statistical post-hoc results, computed by Cohen's d , are reported in Supplementary Materials (4. Details on individual rsEEG data analysis and the statistical results of rsEEG source solutions, Table SM05). The following variables showed a substantial effect size (higher than 0.5): parietal, occipital, and temporal delta source activities; parietal, occipital, and temporal theta source activities; and central alpha 3 source activity.

The above findings were not due to outliers from those individual regional normalized eLORETA current densities (\log_{10} transformed), as shown by Grubbs' test with an arbitrary threshold of $p > 0.001$.

3.2. Individual frequencies and distributions of rsEEG source activities in the alpha-reactive Healthy and alpha-reactive ADMCI groups

The mean TF was 5.7 Hz (± 0.1 SE) in the alpha-reactive Healthy

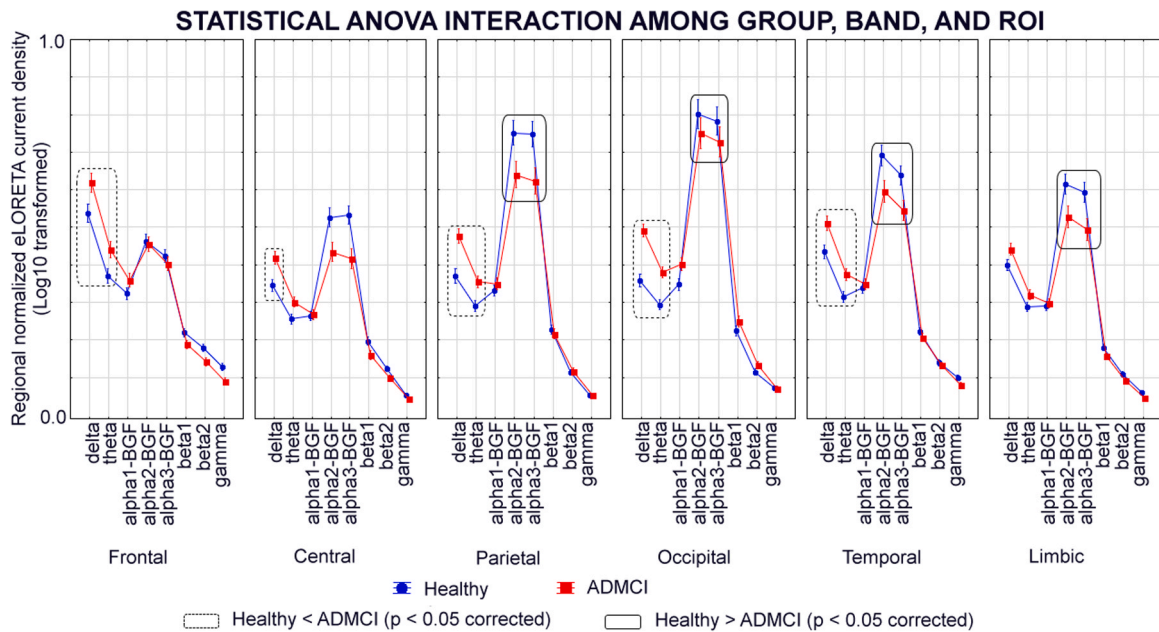


Fig. 2. The rectangles indicate the ROIs and frequency bands in which the eLORETA solutions showed statistically significant effects on Healthy \neq ADMCI ($p < 0.05$ Bonferroni corrected). Legend: alpha background frequency 1, 2, and 3 (alpha-BGF1, alpha-BGF2, and alpha-BGF3). (a) Regional normalized eLORETA solutions (mean across subjects, log 10 transformed) estimating cortical sources of eyes-closed rsEEG rhythms in Healthy and Alzheimer’s disease mild cognitive impairment (ADMCI) groups. (b) These rsEEG source estimates refer to a statistical ANOVA interaction among the factors Group (Healthy, $N = 60$; ADMCI, $N = 52$), Band (delta, theta, alpha-BGF1, alpha-BGF2, and alpha-BGF3, beta1, beta2, and gamma), and Region of Interest, ROI (frontal, central, parietal, occipital, temporal, and limbic).

group ($N = 55$) and 5.2 Hz (± 0.2 SE) in the alpha-reactive ADMCI group ($N = 39$, 75% of the whole group of the ADMCI patients). Furthermore, the mean BGF was 9.1 Hz (± 0.1 SE) in the alpha-reactive Healthy group and 9.0 Hz (± 0.2 SE) in the alpha-reactive ADMCI group. The T-tests of these data showed that the mean TF was greater in the Healthy than in the ADMCI groups ($p < 0.01$). No statistically significant difference was found for the mean BGF ($p > 0.05$).

The results of the second statistical session about the eyes-closed rsEEG source activities in the alpha-reactive participants are illustrated in Figure 3. It shows the mean values (\pm SE, log 10 transformed) of the regional rsEEG (eLORETA) source activities during the eyes-closed condition in the alpha-reactive Healthy group ($N = 55$) and the alpha-reactive ADMCI group ($N = 39$). The distribution of those source activities differed across the Groups, the ROIs, and the Bands. Compared

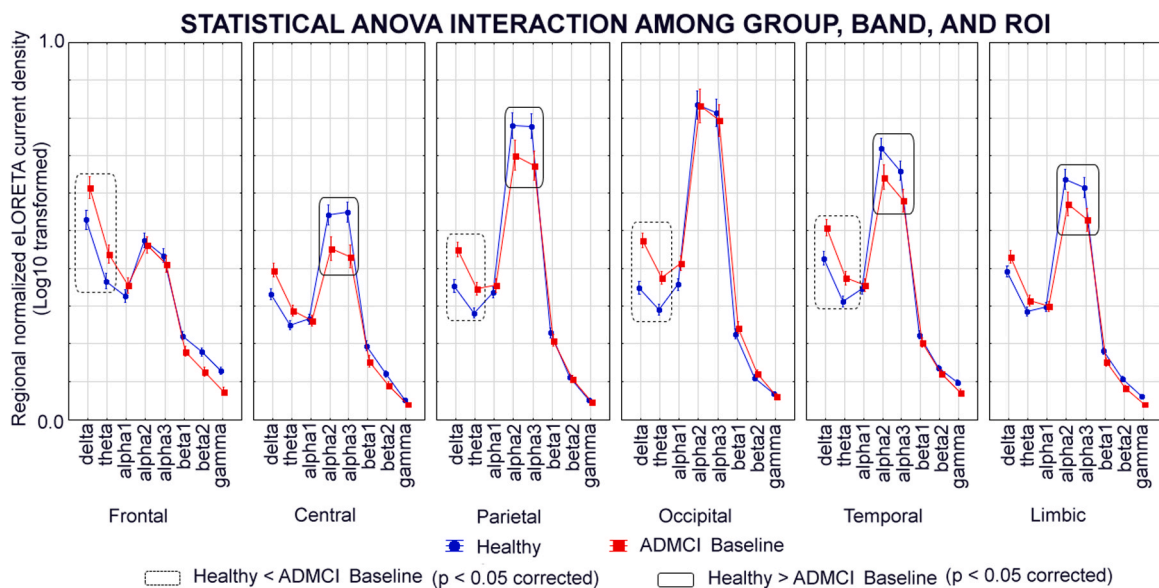


Fig. 3. The alpha reactivity threshold was set at $\geq -10\%$. The rectangles indicate the cortical regions and frequency bands in which the eLORETA solutions showed statistically significant effects on alpha-reactive Healthy \neq alpha-reactive ADMCI ($p < 0.05$ Bonferroni corrected). (a) Regional normalized eLORETA solutions (mean across subjects, log 10 transformed) estimating cortical sources of eyes-closed rsEEG rhythms in alpha-reactive Healthy and ADMCI groups. (b) These rsEEG source estimates refer to a statistical ANOVA interaction among the factors Group (alpha-reactive Healthy, $N = 55$; alpha-reactive ADMCI, $N = 39$), Band (delta, theta, alpha 1, alpha 2, alpha 3, beta 1, beta 2, and gamma), and ROI (frontal, central, parietal, occipital, temporal, and limbic).

to the alpha-reactive Healthy group, the alpha-reactive ADMCI group exhibited a substantial decrease in central, parietal, temporal, and limbic rEEG alpha 2 and alpha 3 source activities. Furthermore, the ADMCI group exhibited increased widespread delta and theta source activities. Based on these input data, the ANOVA results showed a statistical interaction effect ($F(35, 3220) = 2.7, p < 0.00001$) among the following factors: Group (Healthy and ADMCI), Band (delta, theta, alpha 1, alpha 2, alpha 3, beta 1, beta 2, and gamma), and ROI (frontal, central, parietal, occipital, temporal, and limbic). The Duncan planned post-hoc ($p < 0.05$ Bonferroni correction for 8 Bands X 6 ROIs, $p < 0.05/48 = 0.001$) testing produced the following core results: (1) the discriminant pattern Healthy < ADMCI was fitted by the frontal, central, parietal, occipital, and temporal delta source activities ($p < 0.001-0.000001$) as well as the frontal, parietal, occipital, and temporal theta source activities ($p < 0.0001 - 0.000001$); and (2) the discriminant pattern Healthy > ADMCI was fitted by the central, parietal, temporal, and limbic alpha 2 source activities ($p < 0.0005 - 0.00001$) as well as the central, parietal temporal, and limbic alpha 3 source activities ($p < 0.00001 - 0.000005$). The effect size of these statistical post-hoc results, computed by Cohen's d, is reported in [Supplementary Materials \(4. Details on individual rsEEG data analysis and the statistical results of rsEEG source solutions, Table SM06\)](#). The following variables showed a substantial effect size (higher than 0.5): central, parietal, occipital, and temporal delta source activities; parietal, occipital, and temporal theta source activities; central alpha 3 source activity.

These above findings were not due to outliers from those individual regional normalized eLORETA current densities (log 10 transformed), as shown by Grubbs' test with an arbitrary threshold of $p > 0.001$.

3.3. Individual frequencies and distributions of rsEEG source activities in the 6-month follow-up alpha-reactive ADMCI group

In the 6-month follow-up alpha-reactive ADMCI group ($N = 32$), the mean TF was 5.1 Hz (± 0.1 SE) at the baseline and 5.3 Hz (± 0.2 SE) at the 6-month follow-up. Furthermore, the mean BGF was 9.1 Hz (± 0.1 SE) at the baseline and 8.7 Hz (± 0.2 SE) at the 6-month follow-up. No statistically significant difference was found for the mean TF and the

mean BGF (T-test, $p > 0.05$).

The results of the third statistical session about the eyes-closed rsEEG source activities in the 6-month follow-up alpha-reactive ADMCI ($N = 32$) are illustrated in [Figure 4](#). This Figure shows the mean values (\pm SE, log 10 transformed) of the regional rsEEG (eLORETA) source activities during the eyes-closed condition at the baseline and the 6-month follow-up in the alpha-reactive ADMCI group ($N = 32$). The distribution of those source activities differed across the Time, the ROIs, and the Bands. The 6-month follow-up alpha-reactive ADMCI group exhibited a substantial decrease in posterior rsEEG alpha 2 and alpha 3 source activities as well as temporal beta 1 and beta 2 source activities after 6 months. Furthermore, the 6-month follow-up alpha-reactive ADMCI group exhibited an increase in frontal, central, and parietal delta and theta source activities after 6 months. Based on these input data, the ANOVA results showed a statistical interaction effect ($F(35, 1085) = 1.6, p < 0.006$) among the factors Time (Baseline and Follow-up), Band (delta, theta, alpha 1, alpha 2, alpha 3, beta 1, beta 2, and gamma), and ROI (frontal, central, parietal, occipital, temporal, and limbic). The Duncan planned post-hoc ($p < 0.05$ Bonferroni correction for 8 Bands X 6 ROIs, $p < 0.05/48 = 0.001$) testing produced the following core results: (1) the discriminant pattern Baseline < Follow-up was fitted by the frontal, central, and parietal delta source activities ($p < 0.0001 - 0.000005$) as well as the central and parietal theta source activities ($p < 0.0005 - 0.0001$); and (2) the discriminant pattern Baseline > Follow-up was fitted by: (i) the central, parietal, occipital, temporal, and limbic alpha 2 source activities ($p < 0.00005 - 0.00001$); (ii) the central, occipital, parietal temporal, and limbic alpha 3 source activities ($p < 0.0001 - 0.00001$); (iii) the temporal beta 1 source activity ($p < 0.00001$); and (iv) temporal beta 2 source activity ($p < 0.0001$). The effect size of these statistical post-hoc results, computed by Cohen's d, is reported in [Table 3](#). The following variables showed a small effect size (higher than 0.2): frontal, central, and parietal delta source activities; central and parietal theta source activities. Other variables showed small to medium size effects (from 0.2–0.5): central, parietal, occipital, temporal, and limbic alpha 2 and alpha 3 source activities. Finally, the temporal beta 1 and beta 2 source activities showed medium to large size effects (higher than 0.7).

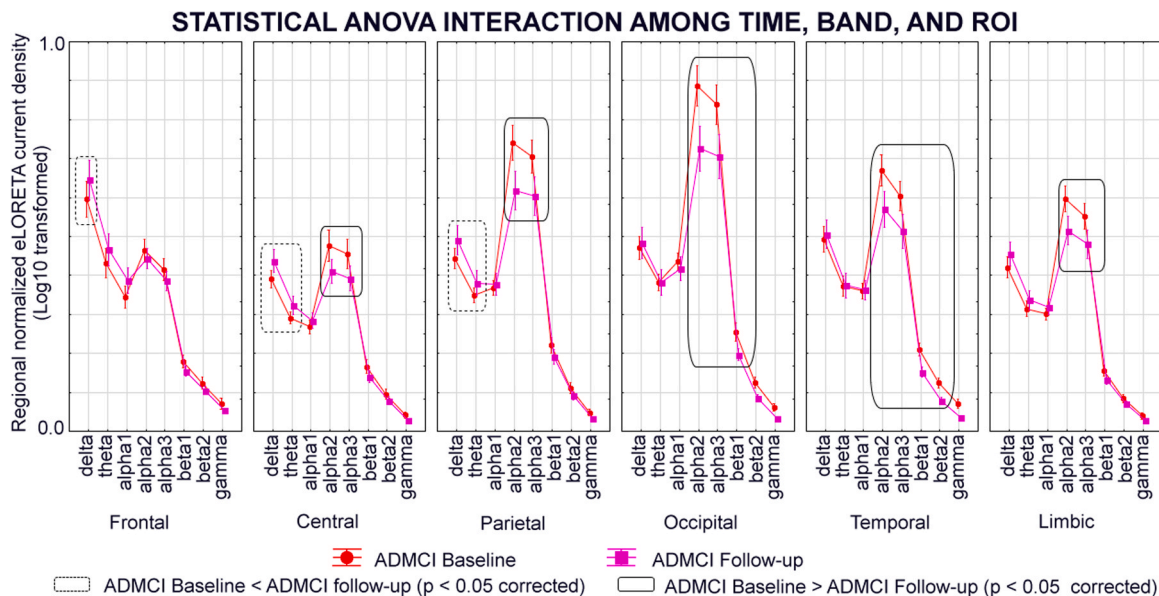


Fig. 4. The alpha reactivity threshold was set at $\geq -10\%$. The rectangles indicate the cortical regions and frequency bands in which the eLORETA solutions showed statistically significant effects on pattern alpha-reactive Baseline \neq 6-month Follow-up ($p < 0.05$ Bonferroni corrected).

(a) Regional normalized eLORETA solutions (mean across subjects, log 10 transformed) estimating cortical sources of eyes-closed rsEEG rhythms in the ADMCI group alpha-reactive ($N = 32$) at the baseline and the 6-month follow-up. (b) These rsEEG source estimates refer to a statistical ANOVA interaction among the factors Time (Baseline and 6-month Follow-up), Band (delta, theta, alpha 1, alpha 2, alpha 3, beta 1, beta 2, and gamma), and ROI (frontal, central, parietal, occipital, temporal, and limbic).

Table 3
Duncan post-HOC comparisons, Cohen's d effect size.

		ADMCI BASELINE vs ADMCI FOLLOW-UP ALPHA-REACTIVE
Delta	Frontal	p < 0.0002, - 0.18
	Central	p < 0.0009, - 0.32
	Parietal	p < 0.0008, - 0.26
	Occipital	-
	Temporal	-
Theta	Frontal	-
	Central	p < 0.001, - 0.28
	Parietal	p < 0.001, - 0.22
	Occipital	-
	Temporal	-
Alpha 2	Frontal	-
	Central	p < 0.000003, 0.34
	Parietal	p < 0.000004, 0.46
	Occipital	p < 0.000003, 0.53
	Temporal	p < 0.000005, 0.41
Alpha 3	Frontal	-
	Central	p < 0.000005, 0.33
	Parietal	p < 0.000004, 0.40
	Occipital	p < 0.000004, 0.44
	Temporal	p < 0.000004, 0.40
Beta 1	Frontal	-
	Central	-
	Parietal	-
	Occipital	p < 0.00001, 0.53
	Temporal	-
Beta 2	Frontal	-
	Central	-
	Parietal	-
	Occipital	p < 0.001, 0.70
	Temporal	p < 0.001, 0.74
	Limbic	-

Table 3: The size effect (Cohen's d) of the statistically significant post-hoc results of the ANOVA interaction among the factors Time (ADMCI Baseline and 6-month follow-up), Band (delta, theta, alpha 1, alpha 2, alpha 3, beta 1, beta 2, gamma), and Region of interest (ROI; frontal, central, parietal, occipital, temporal, and limbic). Legend: ADMCI = Alzheimer's Disease due to Mild cognitive impairment; F= frontal, C= central, P = parietal, O= occipital, T = temporal, and L= limbic.

The above findings were not due to outliers from those individual regional normalized eLORETA current densities (log 10 transformed), as shown by Grubbs' test with an arbitrary threshold of $p > 0.001$.

3.4. Control analyses

The results of the first control analysis showed a statistically significant ANOVA interaction effect ($F(7, 217) = 5.69$; $p = 0.00001$) between the factors Time (ADMCI Baseline and 6-month Follow-up) and Band (delta, theta, alpha1, alpha2, alpha3, beta1, beta2 and gamma) on the rsEEG source activities related to the eyes-closed condition in the alpha-reactive ADMCI group at the baseline and 6-month follow-up ($N = 32$). The alpha-reactive threshold was set at $\geq -10\%$. Compared to the baseline, the 6-month follow-up showed lower rsEEG alpha2 and alpha3 source activities (Figure 5).

The Duncan planned post-hoc testing ($p < 0.05$ Bonferroni correction for 8 frequency bands, $p < 0.05/8 = 0.006$) showed that (1) the discriminant pattern ADMCI baseline $>$ 6-month follow-up was fitted by the rsEEG alpha2 ($p = 0.0002$) and alpha3 ($p = 0.001$) source activities. These findings were not due to outliers from those individual eLORETA solutions (log10 transformed), as shown by Grubbs' test with an arbitrary threshold of $p > 0.001$.

A second control analysis showed the eyes-closed rsEEG source activities in the ADMCI group alpha-reactive at baseline and 6-month

follow-up ($N = 32$). The threshold was set at $\geq -15\%$. There was a statistically significant ANOVA interaction effect ($F = (7, 196) = 4.96$; $p = 0.00003$) between the factors Time (ADMCI Baseline and 6-month Follow-up), and Band (delta, theta, alpha 1, alpha 2, alpha 3, beta 1, beta 2, and gamma). The Duncan planned post-hoc testing ($p < 0.05$ Bonferroni correction for 8 frequency bands, $p < 0.05/8 = 0.0062$) showed the following results (Figure 6): (1) the discriminant pattern ADMCI baseline $<$ 6-month follow-up was fitted by higher rsEEG delta ($p = 0.0054$) source activity and (2) the discriminant pattern ADMCI baseline $>$ 6-month follow-up was fitted by lower rsEEG alpha 2 ($p = 0.0009$) source activities. These findings were not due to outliers from those individual eLORETA solutions (log10 transformed), as shown by Grubbs' test with an arbitrary threshold of $p > 0.001$.

A third control analysis showed the eyes-closed rsEEG source activities in the 6-month follow-up in the alpha-reactive ADMCI ($N = 32$). The threshold was set at $\geq -20\%$. There was a statistically significant ANOVA interaction effect ($F = (7, 189) = 4.42$; $p = 0.00010$) between the factors Time (ADMCI Baseline and 6-month Follow-up) and Band (delta, theta, alpha 1, alpha 2, alpha 3, beta 1, beta 2 and gamma). The Duncan planned post-hoc testing ($p < 0.05$ Bonferroni correction for 8 frequency bands, $p < 0.05/8 = 0.0062$) showed the following results (Figure 7): (1) the discriminant pattern ADMCI baseline $>$ 6-month follow-up was fitted by the alpha 2 ($p = 0.0006$) source activities. These findings were not due to outliers from those individual eLORETA solutions (log10 transformed), as shown by Grubbs' test with an arbitrary threshold of $p > 0.001$.

A fourth control analysis ($p < 0.05$ corrected) was performed to evaluate whether the alpha-reactive Healthy ($N = 55$), alpha-reactive ADMCI (Baseline and 6-month Follow-up, $N = 32$), and alpha no-reactive ADMCI group (Baseline and 6-month Follow-up, $N = 13$) may display some differences in the rsEEG alpha source activity estimated for the eyes-closed condition. Figure 8 shows the regional rsEEG source activities (i.e., regional normalized eLORETA solutions, log 10 transformed) for a statistically significant ANOVA interaction effect ($F(70, 3640) = 5.4$; $p = 0.00001$) among the factors Group (Healthy reactive, ADMCI reactive, and ADMCI no-reactive), Band (delta, theta, alpha 1, alpha 2, alpha 3, beta 1, beta 2, and gamma), and ROI (frontal, central, parietal, occipital, temporal, and limbic). The Duncan planned post-hoc testing ($p < 0.05$ Bonferroni correction for 8 frequency bands X 6 ROIs = 25, $p < 0.05/48 = 0.0010$) showed the following results (Figure 8): (1) the discriminant pattern Healthy alpha-reactive $>$ ADMCI alpha-reactive $>$ ADMCI alpha no-reactive was fitted by the parietal ($p = 0.0002$) alpha2 and ($p = 0.00001$) alpha3 source activities. (2) the discriminant pattern Healthy reactive $<$ ADMCI reactive $<$ ADMCI no-reactive was fitted by the parietal ($p < 0.00001$) delta source activities. These findings were not due to outliers from those individual eLORETA solutions (log 10 transformed), as shown by Grubbs' test with an arbitrary threshold of $p > 0.001$.

We also compared demographical data, clinical data, the Body Mass Index (BMI), the absence or presence of sleep disturbances, the absence or presence of neuropsychiatric disorders (Neuropsychiatric Inventory; NPI), the genetic markers (APOE4), and cerebrospinal fluid markers between the alpha-reactive and alpha no-reactive ADMCI groups, considering the baseline and 6-month follow-up recordings. We have found no statistically significant differences between them considering the mentioned variables ($p < 0.05$; see Table 4). Moreover, we found no statistically significant differences between the two groups for almost all neuropsychological test scores ($p < 0.05$; see Table 5). Interestingly, we had a significant difference between the two groups only on the Clock drawing test ($p < 0.05$), in which the scores were better in the alpha-reactive than alpha-no-reactive ADMCI patients.

A fifth control analysis was performed to evaluate whether the alpha-no-reactive ADMCI group ($N = 13$) may display some differences in the rsEEG source activities estimated for the eyes-closed condition between the baseline and 6-month follow-up. There was a statistically significant ANOVA interaction effect ($F(35, 315) = 1.69$; $p = 0.010$) among the

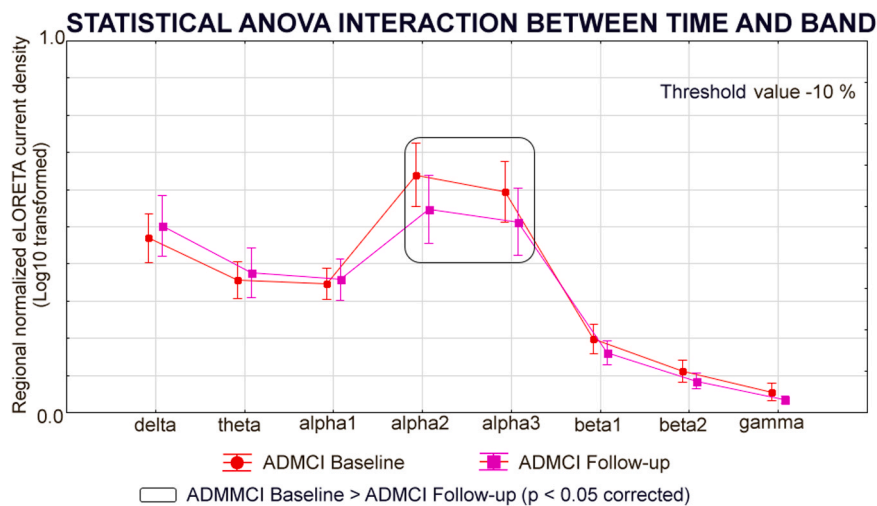


Fig. 5. The alpha reactivity threshold was set at $\geq -10\%$. For a control purpose, the alpha band was obtained including alpha 2 and alpha 3 sub-bands. The rectangles indicate the recording session (Baseline and 6-month Follow-up) and frequency bands in which the eLORETA solutions showed statistically significant effects on pattern Baseline \neq 6-month Follow-up ($p < 0.05$ Bonferroni corrected).

(a) Regional normalized eLORETA solutions (mean across subjects, log 10 transformed) estimating cortical sources of eyes-closed rsEEG rhythms in the ADMCI group alpha-reactive ($N = 32$) at the baseline and the 6-month follow-up. (b) These rsEEG source estimates refer to a statistical ANOVA interaction between the factors Time (Baseline and Follow-up) and Band (delta, theta, alpha, beta, and gamma).

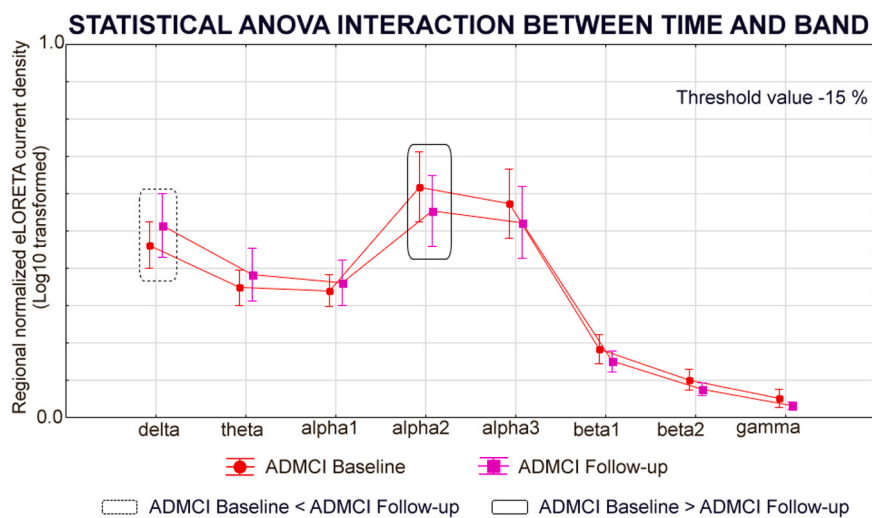


Fig. 6. The alpha reactivity threshold was set at -15% . The rectangles indicate the recording session (Baseline and 6-month Follow-up) and frequency bands in which the eLORETA solutions showed statistically significant effects on pattern Baseline \neq 6-month Follow-up ($p < 0.05$ Bonferroni corrected).

(a) Regional normalized eLORETA solutions (mean across subjects, log 10 transformed) estimating cortical sources of eyes-closed rsEEG rhythms in the ADMCI group alpha-reactive ($N = 32$) at the baseline and the 6-month follow-up. (b) These rsEEG source estimates refer to a statistical ANOVA interaction between the factors Time (Baseline and Follow-up) and Band (delta, theta, alpha, beta, and gamma).

factors Group (ADMCI no-reactive Baseline, and ADMCI no-reactive Follow-up 6 month), Band (delta, theta, alpha 1, alpha 2, alpha 3, beta 1, beta 2 and gamma), and ROI (frontal, central, parietal, occipital, temporal, and limbic). The Duncan planned post-hoc testing ($p < 0.05$ Bonferroni correction for 8 frequency bands \times 6 ROIs = 25, $p < 0.05/48 = 0.0010$) showed only the following results (Figure 9): the discriminant pattern Baseline $<$ 6-month follow-up in the ADMCI alpha-no-reactive group was fitted by higher frontal ($p = 0.00009$), central ($p = 0.00007$), and limbic ($p = 0.0002$) delta source activities and higher frontal ($p = 0.0002$) and limbic ($p = 0.0009$) theta source activities. These findings were not due to outliers from those individual eLORETA solutions (log 10 transformed), as shown by Grubbs' test with an arbitrary threshold of $p > 0.001$.

A sixth control analysis ($p < 0.05$) in the ADMCI group alpha reactive at the baseline recordings ($N = 39$) was performed to evaluate

whether the posterior rsEEG alpha 2 source activities for the eyes-closed condition were correlated with the rsEEG alpha reactivity (Eyes Open – Eyes Closed /Eyes Closed $\times 100$). The posterior region included the central, parietal, and occipital ROIs. Figure 10 shows the scatterplot of the above variables. Results showed a strong linear correlation between the two variables (Pearson $r = -0.6305$; $p = 0.0001$). The higher the posterior rsEEG alpha 2 source activities for the eyes-closed condition, the higher the alpha reactivity from the eyes-closed to the eyes-open condition.

A control analysis ($p < 0.05$ corrected) was performed to evaluate whether the neuropsychological scores may worsen across time (6 months) in the 6-month follow-up in the ADMCI group alpha-reactive at baseline and 6-month follow-up ($N = 32$). For each alpha-reactive ADMCI patient, the procedure was as follows: (1) the neuropsychological tests included the ADAS-Cog, Immediate recall of Rey Auditory

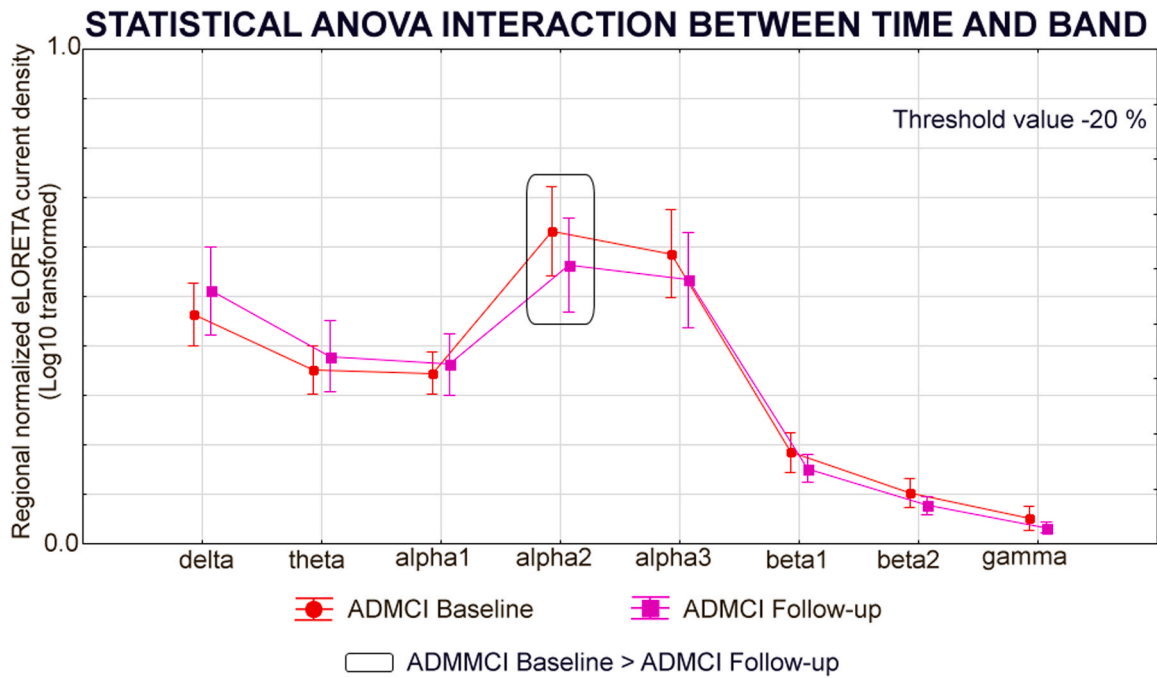


Fig. 7. The alpha reactivity threshold was set at -20% . The rectangles indicate the recording session (Baseline and 6-month Follow-up) and frequency bands in which the eLORETA solutions showed statistically significant effects on pattern Baseline \neq 6-month Follow-up ($p < 0.05$ Bonferroni corrected). (a) Regional normalized eLORETA solutions (mean across subjects, log 10 transformed) estimating cortical sources of eyes-closed rEEG rhythms in the ADMCI group alpha-reactive ($N = 32$) at the baseline and the 6-month follow-up. (b) These rsEEG source estimates refer to a statistical ANOVA interaction between the factors Time (Baseline and Follow-up) and Band (delta, theta, alpha, beta, and gamma).

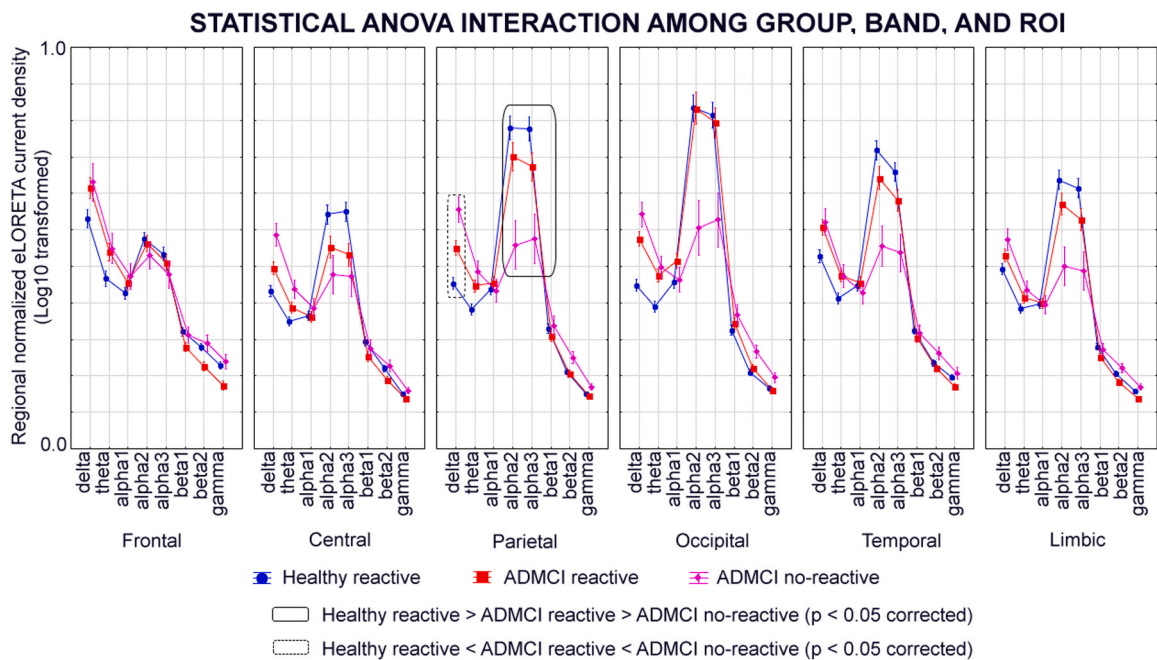


Fig. 8. The alpha reactivity threshold was set at $\geq -10\%$. The rectangles indicate the cortical regions and frequency bands in which the eLORETA solutions showed statistically significant effects on pattern Healthy \neq ADMCI ($p < 0.05$ Bonferroni corrected). (a) Regional normalized eLORETA solutions (mean across subjects, log 10 transformed) estimating cortical sources of eyes-closed rEEG rhythms in Healthy and ADMCI groups. (b) These rsEEG source estimates refer to a statistical ANOVA interaction among the factors Group (Healthy alpha-reactive, $N = 55$; ADMCI alpha-reactive, $N = 32$; ADMCI alpha no-reactive, $N = 10$), Band (delta, theta, alpha 1, alpha 2, and alpha 3, beta 1, beta 2, and gamma), and ROI (central, frontal, parietal, occipital, temporal, and limbic).

Verbal Learning Test, Delayed recall of Rey Auditory Verbal Learning Test, Verbal fluency test for letters, Verbal fluency test for the category, TMT B-A, and Clock drawing test; (2) the neuropsychological scores were log 10 transformed to make them Gaussian before the subsequent

parametric statistical analysis; (3) t-tests were computed to evaluate the presence or absence of statistically significant differences between the baseline and the 6-month follow-up for the above-mentioned neuropsychological scores. To consider the inflating effects of multiple

Table 4

Demographic, genetic (APOE), and cerebrospinal fluid markers in ADMCI baseline and follow-up 6 M alpha-reactive and ADMCI baseline and follow-up 6 M no-reactive groups.

	ADMCI Baseline and Follow-up 6 M REACTIVE	ADMCI Baseline and Follow-up 6 M NO-REACTIVE	T-test	
	Mean ± SE (% subjects with abnormal score)	Mean ± SE (% subjects with abnormal score)		
N	32	10		
Age	69.84 ± 1.26	67.30 ± 1.81	n.s.	
sex(M/F)	13/19	03/07	n.s. (Fisher test)	
education	11.47 ± 0.80	10.70 ± 1.45	n.s.	
MMSE	26.69 ± 0.30	25.90 ± 0.55	n.s. (Mann-Whitney U- test)	
Sleep disturbances (yes/no)	4/28 (13%)	3/7 (30%)	n.s. (Fisher test)	
NPI (yes/no)	21/11 (66%)	9/1 (90%)	n.s. (Fisher test)	
APOE4 (yes/no)	24/08 (75%)	09/01 (90%)	n.s. (Fisher test)	
BMI	> 25	25.29 ± 0.64 (44%)	24.57 ± 0.84 (50%)	n.s.
A-beta42	< 599	490.46 ± 29.72 (69%)	534.64 ± 31.63 (60%)	n.s.
P- tau	> 56.5	86.66 ± 7.21 (78%)	87.72 ± 11.45 (70%)	n.s.
T- tau	> 404	614.37 ± 61.16 (63%)	613.51 ± 84.82 (70%)	n.s.
Abeta/p- tau	< 8.1	6.57 ± 0.55 (72%)	7.40 ± 1.20 (70%)	n.s.

Table 4. Mean values (± SE) of the demographic (age, sex, educational attainment), genetic (i.e., Apolipoprotein E genotyping, APOE), and cerebrospinal fluid (i.e., beta-amyloid 1-42, Aβ 42; protein tau, t-tau; a phosphorylated form of the protein tau, p-tau; and Aβ 42/ p-tau ratio) data in the Alpha reactive ADMCI group at Baseline and 6-month Follow-up (N = 32) and Alpha no-reactive ADMCI group at Baseline and 6-month Follow-up (N = 10). The cut-off scores and percentage of abnormality of the cerebrospinal fluid markers tests are also reported Legend: M/F = males/females; n.s. = not significant (p > 0.05); MMSE = Mini-Mental State Evaluation; ADMCI Baseline and Follow-up 6 M = patients with mild cognitive impairment due to Alzheimer's disease at Baseline and 6-month follow-up; BMI = Body mass index; NPI = Neuropsychiatric inventory.

univariate tests, the statistical threshold was set at p < 0.007 (i.e., 7 neuropsychological scores, p < 0.05/7 = 0.007) to obtain the Bonferroni correction at p < 0.05. No statistically significant difference was found (p > 0.05; see [Supplementary materials Table SM07](#)).

Another control analysis (p < 0.05 corrected) was performed to evaluate whether the standard structural MRI markers reflecting brain neurodegeneration may worsen at the 6-month follow-up in the ADMCI group alpha reactive at baseline and 6-month follow-up recordings (N = 32). For each alpha-reactive ADMCI patient, the procedure was as follows: (1) the structural MRI markers included (i) the volumes of the hippocampus and lateral ventricle for the left and right hemispheres (these markers were normalized with respect to the total intracranial volume) and (ii) the cortical thicknesses of the para-hippocampal gyrus, fusiform gyrus, entorhinal cortex, precuneus, and cuneus for the left and right hemispheres; (2) the structural MRI markers were log 10 transformed to make them Gaussian before the subsequent parametric

Table 5

Neuropsychological scores in ADMCI baseline and follow-up 6 M alpha-reactive and ADMCI baseline and follow-up 6 M No-reactive groups.

	Cut-off of abnormality	ADMCI Baseline and Follow-up 6 M REACTIVE Mean ± SE (% subjects with abnormal score)	ADMCI Baseline and Follow-up 6 M NO-REACTIVE Mean ± SE (% subjects with abnormal score)	T-test
ADAS-Cog	≥ 17	21.20 ± 1.35 (78%)	24.60 ± 1.75 (80%)	n.s. (fisher test)
Trail Making test B-A	≥ 187	117.53 ± 12.1 (19%)	145.78 ± 22.22 (22%)	n.s.
RAVLT imm. recall	< 28.53	30.53 ± 2.01 (50%)	26.10 ± 2.2 (70%)	n.s.
RAVLT delayed recall	< 4.69	5.25 ± 1.47 (66%)	2.70 ± 0.6 (90%)	n.s.
Clock drawing	< 3	4.03 ± 0.2 (25%)	3.00 ± 0.4 (60%)	P = 0.02
Letter fluency	< 17	33.25 ± 1.78 (3%)	32.10 ± 3.24 (10%)	n.s.
Letter category	< 25	32.19 ± 2.02 (28%)	32.0 ± 3.62 (20%)	n.s.

Table 5. Mean values (± SE) of the neuropsychological scores (i.e., ADAS-Cog, Rey Auditory Verbal Learning Test immediate recall, Rey Auditory Verbal Learning Test delayed recall, Trail Making Test part B-A, Verbal fluency for letters, Verbal fluency for category, Clock drawing) as well as the results of their statistical comparisons (T-test; p < 0.05) in the groups of ADMCI Alpha-reactive (N = 32) and ADMCI Alpha no-reactive (N = 10) patients. The cut-off scores of the neuropsychological tests are also reported. Legend: ADMCI Baseline and Follow-up 6 M = patients with mild cognitive impairment due to Alzheimer's disease at Baseline and 6-month Follow-up; ADAS-Cog = Alzheimer's Disease Assessment Scale-Cognitive Subscale; RAVLT = Rey Auditory Verbal Learning Test; TMT B-A = Trail Making Test part B-A.

statistical analysis; (3) t-tests were computed to evaluate the presence or absence of statistically significant differences between the baseline and the 6-month follow-up for the above-mentioned structural MRI markers. To consider the inflating effects of multiple univariate tests, the statistical threshold was set at p < 0.00357 (i.e., 14 MRI markers, p < 0.05/16 = 0.00357) to obtain the Bonferroni correction at p < 0.05. Statistically significant differences (p < 0.05 corrected) showed significantly lower values of the following structural MRI-based variables at the 6-month follow-up than the baseline: (1) the volumes of the left hippocampus, left lateral ventricle, and right lateral ventricle and (2) the cortical thickness of the left entorhinal cortex and the right entorhinal cortex (see [Supplementary materials Table SM08](#)). These results confirmed the progression of AD-related neurodegeneration in the alpha-reactive ADMCI patients at the 6-month follow-up.

4. Discussion

In this study, we tested the hypothesis that in ADMCI patients showing a consistent magnitude of rsEEG alpha rhythms in the eyes-closed condition and a substantial reactivity in the transition to the eyes-open condition (defined as ≥ -10%), the posterior rsEEG alpha rhythms during the eyes-closed condition may be sensitive to the disease progression at the 6-month follow-up. Such a threshold of alpha reactivity was arbitrary and was set to tackle the large variability in the rsEEG alpha rhythms and their reactivity during the eyes-open condition.

The main results showed that in the baseline recordings, there was a substantial (≥ -10%) reduction in the posterior rsEEG alpha source

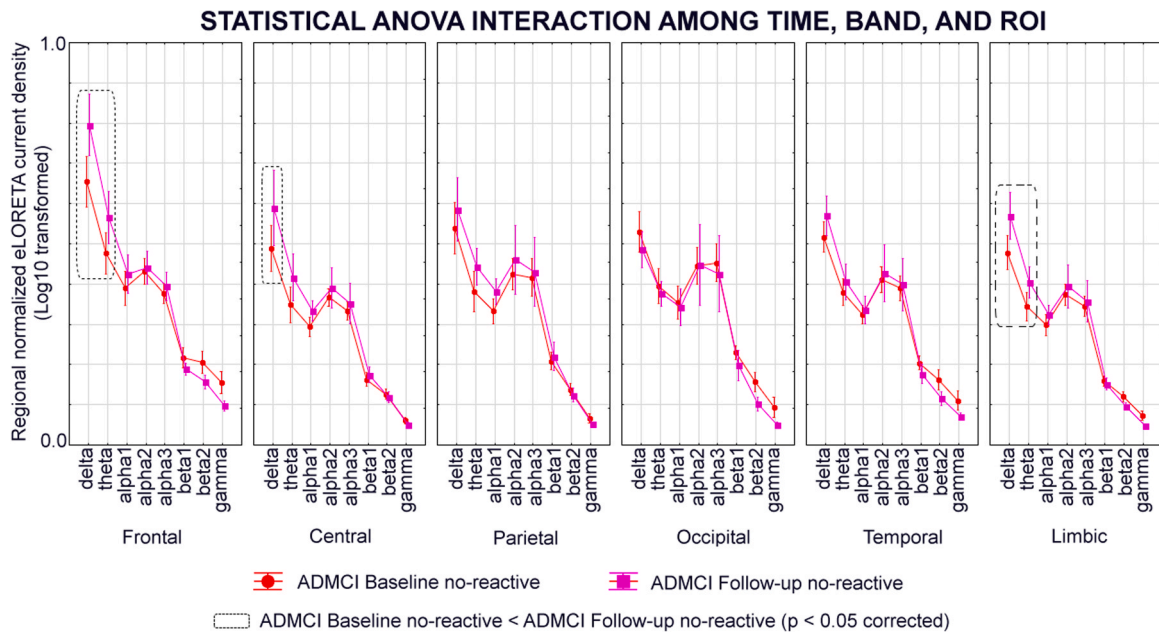


Fig. 9. The alpha reactivity threshold was set at $\geq -10\%$. The rectangles indicate the cortical regions and frequency bands in which the eLORETA solutions showed statistically significant effects on pattern alpha-reactive Baseline \neq 6-month Follow-up ($p < 0.05$ Bonferroni corrected). (a) Regional normalized eLORETA solutions (mean across subjects, log 10 transformed) estimating cortical sources of eyes-closed rEEG rhythms in the ADMCI group no-alpha-reactive ($N = 13$) at the baseline and the 6-month follow-up. (b) These rEEG source estimates refer to a statistical ANOVA interaction among the factors Time (Baseline and 6-month Follow-up), Band (delta, theta, alpha 1, alpha 2, alpha 3, beta 1, beta 2, and gamma), and ROI (central, frontal, parietal, occipital, temporal, and limbic).

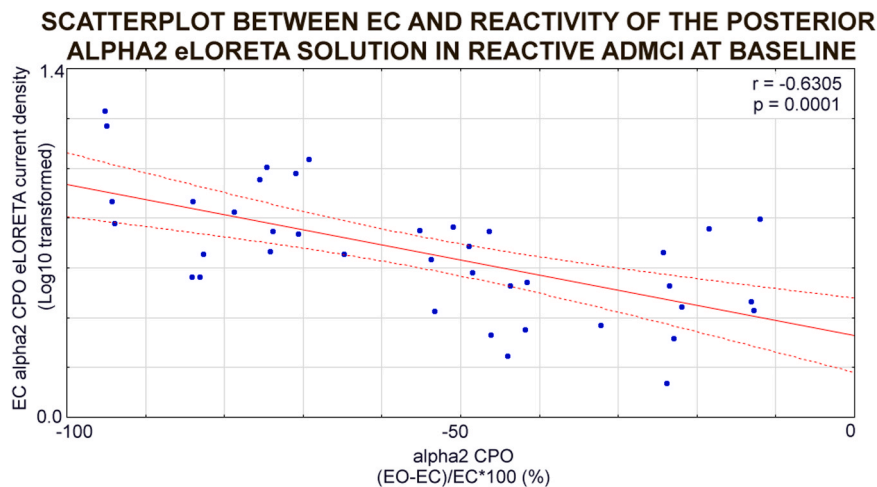


Fig. 10. Scatterplot showing the correlation between regional normalized eLORETA solutions estimating cortical sources of eyes-closed rEEG alpha 2 rhythms in the central, parietal, and occipital ROIs and the reactivity of those source activity (EO-EC/EC*100) in the alpha-reactive ADMCI patients ($N = 39$) at the Baseline recordings. Spearman test confirmed a statistically significant correlation between these two variables ($p < 0.05$). Legend: CPO= central, parietal, and occipital ROIs; EC = Eyes Closed.

activities during the eyes-open condition in about 90% and 75% of Healthy and ADMCI participants, respectively. Therefore, the alpha reactivity threshold set at $\geq -10\%$ may be used in most ADMCI patients to reduce the variability of the dominant posterior rEEG alpha source activity.

The core study results in the alpha-reactive ADMCI patients showed that the higher the dominant posterior rEEG alpha rhythms during the eyes-closed condition, the higher the reactivity of the rEEG alpha rhythms during the eyes-open condition, and the higher the reduction of the rEEG alpha rhythms during the eyes-closed condition at the 6-month follow-up. These results indicate that an arbitrary rEEG alpha-reactivity threshold of $\geq -10\%$ allows us to probe the effects of AD

progression over 6 months on dominant posterior rEEG alpha rhythms during the eyes-closed condition. Along this line, they complement and extend previous studies showing that posterior rEEG alpha rhythms during eyes-closed condition were relatively stable over months in healthy adults (Salinsky et al., 1991; Kondacs and Szabó, 1999; Näpflin et al., 2007; Duan et al., 2020) and were reduced in magnitude at follow-ups of ≥ 1 year in ADMCI patients (Jelic et al., 2000; Babiloni et al., 2013b).

4.1. Speculative lines for the interpretation of the results

The methodological limitations of the present exploratory study do

not allow us to draw definite conclusions. We can only speculate on the neurophysiological interpretation of the results. Specifically, we propose three lines of speculation. In the first speculative line, we posit that in the alpha-reactive ADMCI patients, the magnitude reduction of rsEEG alpha rhythms during the eyes-closed condition at the 6-month follow-up may impact AD progression on the patients' vigilance level in quiet wakefulness. Along this line, a previous study used a continuous reaction time task in healthy adults (Jagannathan et al., 2019). They responded to the stimuli regularly and fast during the first minutes of the task, in association with ample pre-stimulus dominant posterior rsEEG alpha rhythms (Jagannathan et al., 2019). As time progressed in the experiment, the reaction times became more variable, and the participants intermittently failed to respond in association with reduced pre-stimulus rsEEG alpha rhythms (Jagannathan et al., 2019). In another study, posterior rsEEG alpha rhythms become intermittent and less shaped during the transition of vigilance to drowsiness and light sleep (Tanaka et al., 1996). Furthermore, an experiment using one night of sleep deprivation showed decreased posterior rsEEG alpha (8–13 Hz) rhythms in healthy adults (Del Percio et al., 2019). In another condition of the same experiment, an acute administration of a vigilance enhancer (modafinil) immediately after such sleep deprivation partially recovered those alpha rhythms (Del Percio et al., 2019). Notably, in the present resting-state condition, dominant posterior rsEEG alpha rhythms during the eyes-closed condition may be minimally reflecting other neurophysiological mechanisms previously associated with the EEG alpha activity, namely to gate information processing and transfer during focused attention, sensory processes, information retrieval from long-term memory, goal-oriented reasoning, and motor responses. In event-related conditions, these mechanisms underly the inhibition of task-irrelevant information processing in neural populations, enhance sensory discrimination as a function of alpha phases and frequency, underpin feedback from secondary to primary sensory areas, and stabilize percepts (Klimesch, 1999; Pfurtscheller and Lopes da Silva, 1999; Pineda, 2005; Jensen and Mazaheri, 2010; Başar, 2012; Clayton et al., 2018).

In the second speculative line, we propose that the above magnitude reduction of rsEEG alpha rhythms may reflect the AD progression effects on the neuromodulatory subcortical ascending systems regulating cortical arousal in the quiet wakefulness, including thalamus-cortical reciprocal loops and circuits originating from the cholinergic basal forebrain to the posterior cerebral cortex (Pfurtscheller and Lopes da Silva, 1999; Babiloni et al., 2013a; Wan et al., 2019). Along this line, a previous study in healthy adults showed the relationship between the amplitude of the posterior rsEEG alpha rhythms and cortical arousal, unveiling the negative correlation between such amplitude and skin conductance levels denoting autonomic arousal (Barry et al., 2020). Another study in healthy adults reported that a few seconds of transcranial vagal-nerve electric stimulations (over sham stimulations) caused transient pupil dilation and attenuation in occipital rsEEG alpha rhythms, as expected based on the known effects of vagal nerve stimulation on nucleus tractus solitarius of the brainstem and, consequently, locus coeruleus, which belongs to the neuromodulatory subcortical arousing systems (Joshi et al., 2016; Sharon et al., 2021). Furthermore, inhibiting the occipital cortex by transcranial static magnetic field stimulations induced a local increase in the rsEEG rhythms and, in a separate session, a slowing in visual search (Gonzalez-Rosa et al., 2015). Notably, ample rsEEG alpha rhythms, reflecting cortical inhibition, reduced the propagating effects of short transcranial magnetic stimulations over the dorsal premotor cortex through local action potentials and related blood oxygen level-dependent (BOLD) signal of resting-state functional MRI (rs-fMRI) across the bilateral cortico-subcortical (striatum- thalamus) motor systems (Peters et al., 2020). Another study showed that in healthy old adults, BOLD signal measures of functional connectivity between cholinergic basal forebrain and occipital cortical areas were higher from the eyes-closed to the eyes-open condition in association with the rsEEG alpha reactivity (Wan et al., 2019). In the

same study, lesions in structural MRI-based measures of subcortical white-matter connectivity between cholinergic basal forebrain and occipital cortical areas were associated with a reduction in rsEEG alpha reactivity (Wan et al., 2019). In other studies, there was a positive association between the rsEEG alpha rhythms during the eyes-closed condition and the BOLD signal in the thalamus and mainly a negative association in the visual and attention posterior cerebral cortex in quiet wakefulness, suggesting that those alpha rhythms may reflect a cortical inhibition induced by thalamocortical signaling to regulate cortical arousal (de Munck et al., 2007; Laufs et al., 2006; Olbrich et al., 2009; Knaut et al., 2019). Furthermore, ADD patients over healthy controls were characterized by decreased associations between the rsEEG alpha rhythms and the BOLD signal in cortical areas and the thalamus (Brueggen et al., 2017).

Concerning the potential contribution of the cholinergic ascending system, it was previously shown that the dominant posterior rsEEG alpha rhythms in healthy adults decreased in amplitude after acute administrations of cholinergic antagonist scopolamine as a dementia model, following its pharmacodynamic course (see a review in Ebert and Kirch, 1998). Furthermore, those rsEEG alpha rhythms were especially low in magnitude in ADMCI patients, with substantial impairment estimated in the cholinergic tract to posterior cortical areas (Babiloni et al., 2009). Moreover, dominant posterior rsEEG alpha rhythms deteriorated less in magnitude at 1-year follow-ups in ADD patients who clinically responded to the therapy with Acetylcholinesterase inhibitors (Babiloni et al., 2006).

In the third speculative line, we propose that the abnormalities in the above neuromodulatory ascending systems may depend on the progression of AD neuropathology. Along this line, a previous study reported that CSF amyloid β 42, p-tau, and total tau levels linearly correlated with global power or synchronization of rsEEG alpha and beta rhythms in ADMCI and ADD patients (Smailovic et al., 2018). In another study, CSF p-tau and p-tau/A β 42 correlated with rsEEG alpha rhythms in ADD patients (Kouzuki et al., 2013). Other studies showed more abnormal rsEEG alpha rhythms in MCI groups positive than negative to CSF biomarkers of AD (Jovicich et al., 2019; Cecchetti et al., 2021). Furthermore, significant associations were observed between AD neuropathology and slowing in frequencies of rsEEG alpha rhythms recorded in AD patients. More abnormal CSF amyloid β 42/p-tau values were related to slower frequencies of these rhythms in persons with ADD, ADMCI, mixed dementia, and subjective cognitive impairment (Kramberger et al., 2013). These findings were globally confirmed in cognitively unimpaired, ADMCI, and ADD persons (Tanabe et al., 2019), thus remarking on the importance of using individual measures of rsEEG alpha rhythms.

4.2. Methodological study limitations

Concerning the methodological study limitations, it should be remarked that no direct physiological measures of cortical arousal and cholinergic/noradrenergic neurotransmissions were taken and correlated with the rsEEG data. Furthermore, the experimental design did not include external stimuli and cognitive-motor demands to provide behavioral measures of vigilance to be correlated with the EEG data. At this early research stage, these demands were not included to not interfere with the scope of the resting-state condition (e.g., induce spontaneous EEG activity). Moreover, the experimental design included neither control rsEEG recordings at the 6-month follow-up in healthy seniors nor multiple follow-ups in the ADMCI patients. Consequently, we could not control the potential influence of the regression on the mean in explaining the changes of rsEEG alpha rhythms over time in ADMCI patients. Finally, another methodological limitation of the present study is the low spatial resolution of the EEG techniques used. Indeed, the rsEEG recordings were performed with the 19 scalp electrodes of the standard clinical 10–20 montage; their position was not digitalized, and the cortical source model was not based on individual

volumetric MRIs. These procedures do not allow accurate rsEEG source localizations (Liu et al., 2002; Marino et al., 2016), so the present rsEEG source activities were estimated in large cortical regions of interest using the popular eLORETA freeware (<https://www.uzh.ch/keyinst/loreta.htm>). This freeware was intrinsically designed to provide optimal spatially smoothed source solutions from rsEEG activity suitable for the present low-resolution rsEEG data (Tait et al., 2021).

Keeping in mind these methodological limitations, we recommended future longitudinal (with more than one follow-up) and multi-center studies performed in ADMCI patients using > 48 scalp electrodes, the digitization of their position, and the integration with cortical source models constructed from individual MRIs for investigating rsEEG source activity and connectivity patterns with higher spatial resolution estimates. With a high-resolution approach, further improvements in the rsEEG source solutions may be obtained by orthogonalization techniques, allowing an attenuation of spatial EEG signal leakage (Colclough et al., 2015). These future studies may validate biomarkers of rsEEG alpha rhythms, probing neurophysiological mechanisms underlying cortical arousal and quiet vigilance. These mechanisms are part of the higher brain functions and are clinically relevant for the quality of life of AD patients, even beyond the global cognitive status per se (Babiloni, 2022). Abnormalities in those mechanisms interfere with the patient's ability to maintain stable, quiet vigilance while watching a TV program or having a quiet social conversation with friends and relatives. Notably, the standard neuropsychological tests measuring focused attention, working/episodic memory, verbal fluency, or global cognitive status in active wakefulness do not directly and accurately probe vigilance regulation in quiet wakefulness. Therefore, neurologists and geriatrics cannot obtain a quantitative measure of brain function from the standard clinical scales and neuropsychological tests used to assess AD patients. The results of those future studies may enlighten the actual dark side of Precision Medicine in AD (Babiloni, 2022) and may realize the dream of the father of EEG a century after the first scientific publication on rsEEG alpha rhythms in humans, Hans Berger (Berger, 1929; Gloor, 1994).

5. Conclusions

Here we tested the exploratory hypothesis that posterior rsEEG alpha rhythms may be sensitive to the ADMCI progression at a 6-month follow-up. The ADMCI patients were arbitrarily divided into two groups: alpha-reactive and alpha-no-reactive, based on the reduction (reactivity) in the posterior rsEEG alpha source activities from the eyes-closed to eyes-open condition at $\geq -10\%$ and $< -10\%$, respectively.

75% of the ADMCI patients were alpha-reactive. Compared to the alpha-no-reactive group, the alpha-reactive group showed (1) less abnormal posterior rsEEG source activity during the eyes-closed condition and (2) a decrease in that activity at the 6-month follow-up. These effects could not be explained by neuroimaging and neuropsychological biomarkers of AD.

These results suggest that in selected (i.e., alpha-reactive) ADMCI patients, the dominant, posterior rsEEG alpha rhythms may deteriorate at the 6-month follow-up as an interesting candidate neurophysiological biomarker for short intervention clinical trials. Such a biomarker might reflect abnormalities in cortical arousal and vigilance in quiet wakefulness.

The present results motivate further investments and research aimed at testing the beneficial heuristic and clinical effects of the inclusion of rsEEG measures in the actual panel for the assessment of AD patients, namely the A-T-N(C) Framework (Jack et al., 2018). Those rsEEG measures may be considered pathophysiological "P" biomarkers in the A-T-N(C) Framework to probe the neurophysiological mechanisms generating rsEEG rhythms, which reflect fundamental mechanisms regulating the synchronization of cortical neural activity and functional connectivity of that activity in the condition of quiet wakefulness. Using a threshold of $\geq -10\%$ in the alpha reactivity is promising for using

rsEEG alpha source activity as a biomarker of disease progression in ADMCI patients in relatively short clinical studies with 6-month follow-ups.

CRedit authorship contribution statement

Claudio Babiloni, Claudio Del Percio, Susanna Lopez, Giuseppe Noce, Federico Tucci, and Dharmendra Jakhar: Conceptualization, Methodology, Formal analysis, Validation, Writing – original draft, Supervision, Writing – review & editing, Project administration. **Andrea Soricelli, Marco Salvatore, Raffaele Ferri, Valentina Catania, Federico Massa, Dario Arnaldi, Francesco Famà, Bahar Güntekin, Görsev Yener, Fabrizio Stocchi, Laura Vacca, Moira Marizzoni, Franco Giubilei, Ebru Yıldırım, Lutfu Hanoglu, Duygu Hünerli Gündüz, Giovanni B. Frisoni:** Investigation, Data curation, Project administration, Writing – review & editing.

Declaration of Competing Interest

None of the authors have potential conflicts of interest to be disclosed.

Acknowledgments

The present study was developed based on the data of The PDWAVES Consortium (www.pdwaves.eu) with some datasets of the FP7-IMI "PharmaCog" (www.pharmacog.org) project. The research activities of the Unit of Sapienza University of Rome were partially supported by the HORIZON 2021, HORIZON-INFRA-2021-TECH-01 (Grant Agreement: GAP-101058516) with the short title "eBRAIN-Health.". The members and institutional affiliations of the Clinical Units are reported on the cover page of this manuscript. The Authors thank Dr. Roberta Lizio (Sapienza University of Sapienza) for her useful input on the project.

Verification

1. (a) No Author has conflicts of interest, including any financial, personal, or other relationships with other people or organizations within three years of beginning the work submitted that could inappropriately influence (bias) their work, or financial disclosures in the development of the present pre-competitive basic neurophysiological research, which was based on EEG recordings in demented patients and normal subjects.

1. (b) None of the author's institutions has contracts relating to this research through which it or any other organization may stand to gain financially now or in the future.

1. (c) Authors state that there are no other agreements of authors or their institutions that could be seen as involving a financial interest in this work.

2. The present study was developed based on the data of the informal European Consortia PDWAVES and FP7-IMI "PharmaCog". The members and institutional affiliations of the Consortium are reported on the cover page of this manuscript.

3. Authors state that the data contained in the manuscript being submitted have not been previously published, have not been submitted elsewhere, and will not be submitted elsewhere while under consideration at Neurobiology of Aging.

4. Local institutional Ethical Committees approved the study. All experiments were performed with the informed and overt consent of each participant or caregiver, in line with the Code of Ethics of the World Medical Association (Declaration of Helsinki) and the standards established by the local Institutional Review Board.

5. All the authors reviewed the contents of the manuscript being submitted, approved its contents, and validated the accuracy of the data.

Appendix A. Supporting information

Supplementary data associated with this article can be found in the online version at [doi:10.1016/j.neurobiolaging.2024.01.013](https://doi.org/10.1016/j.neurobiolaging.2024.01.013).

References

- Albert, M.S., DeKosky, S.T., Dickson, D., Dubois, B., Feldman, H.H., Fox, N.C., Gamst, A., Holtzman, D.M., Jagust, W.J., Petersen, R.C., Snyder, P.J., Carrillo, M.C., Thies, B., Phelps, C.H., 2011. The diagnosis of mild cognitive impairment due to Alzheimer's disease: recommendations from the National Institute on Aging-Alzheimer's Association workgroups on diagnostic guidelines for Alzheimer's disease. *Alzheimer's Dement* 7 (3), 270–279. <https://doi.org/10.1016/j.jalz.2011.03.008>. Epub 2011 Apr 21. PMID: 21514249.
- Babiloni, C., 2022. The dark side of alzheimer's disease: neglected physiological biomarkers of brain hyperexcitability and abnormal consciousness level. *J. Alzheimers Dis.* 88 (3), 801–807. <https://doi.org/10.3233/JAD-220582>. PMID: 35754282.
- Babiloni, C., Cassetta, E., Dal Forno, G., Del Percio, C., Ferreri, F., Ferri, R., Lanuzza, B., Miniussi, C., Moretti, D.V., Nobili, F., Pascual-Marqui, R.D., Rodriguez, G., Luca Romani, G., Salinari, S., Zanetti, O., Rossini, P.M., 2006. Donepezil effects on sources of cortical rhythms in mild Alzheimer's disease: Responders vs. Non-Responders. *Neuroimage* 31 (4), 1650–1665. <https://doi.org/10.1016/j.neuroimage.2006.02.015>. Epub 2006 Apr 5. PMID: 16600641.
- Babiloni, C., Pievani, M., Vecchio, F., Geroldi, C., Eusebi, F., Fracassi, C., Fletcher, E., De Carli, C., Boccardi, M., Rossini, P.M., Frisoni, G.B., 2009. White-matter lesions along the cholinergic tracts are related to cortical sources of EEG rhythms in amnesic mild cognitive impairment. *Hum. Brain Mapp.* 30 (5), 1431–1443. <https://doi.org/10.1002/hbm.20612>. PMID: 19097164; PMCID: PMC6871072.
- Babiloni, C., Lizio, R., Vecchio, F., Frisoni, G.B., Pievani, M., Geroldi, C., Claudia, F., Ferri, R., Lanuzza, B., Rossini, P.M., 2010. Reactivity of cortical alpha rhythms to eye-opening in mild cognitive impairment and Alzheimer's disease: an EEG study. *J. Alzheimers Dis.* 22 (4), 1047–1064. <https://doi.org/10.3233/JAD-2010-100798>. PMID: 20930306.
- Babiloni, C., Lizio, R., Del Percio, C., Marzano, N., Soricelli, A., Salvatore, E., Ferri, R., Cosentino, F.L., Tedeschi, G., Montella, P., Marino, S., De Salvo, S., Rodriguez, G., Nobili, F., Vernieri, F., Ursini, F., Mundi, C., Richardson, J.C., Frisoni, G.B., Rossini, P.M., 2013. Cortical sources of resting state EEG rhythms are sensitive to the progression of early-stage Alzheimer's disease. *J. Alzheimers Dis.* 34 (4), 1015–1035. <https://doi.org/10.3233/JAD-121750>. PMID: 23340039.
- Babiloni, C., Del Percio, C., Lizio, R., Noce, G., Cordone, S., Lopez, S., Soricelli, A., Ferri, R., Pascarelli, M.T., Nobili, F., Arnaldi, D., Aarsland, D., Orzi, F., Buttini, C., Giubilei, F., Onofri, M., Stocchi, F., Stirpe, P., Fuhr, P., Gschwandtner, U., Ransmayr, G., Caravias, G., Garn, H., Sorpresi, F., Pievani, M., Frisoni, G.B., D'Antonio, F., De Lena, C., Güntekin, B., Hanoğlu, L., Başar, E., Yener, G., Emek-Savaş, D.D., Triggiani, A.I., Franciotti, R., De Pandis, M.F., Bonanni, L., 2017a. Abnormalities of cortical neural synchronization mechanisms in patients with dementia due to Alzheimer's and Lewy body diseases: an EEG study. *Neurobiol. Aging* 55, 143–158. <https://doi.org/10.1016/j.neurobiolaging.2017.03.030>. Epub 2017 Apr 5. PMID: 28454845.
- Babiloni, C., Del Percio, C., Lizio, R., Noce, G., Cordone, S., Lopez, S., Soricelli, A., Ferri, R., Pascarelli, M.T., Nobili, F., Arnaldi, D., Famà, F., Aarsland, D., Orzi, F., Buttini, C., Giubilei, F., Onofri, M., Stocchi, F., Stirpe, P., Fuhr, P., Gschwandtner, U., Ransmayr, G., Caravias, G., Garn, H., Sorpresi, F., Pievani, M., D'Antonio, F., De Lena, C., Güntekin, B., Hanoğlu, L., Başar, E., Yener, G., Emek-Savaş, D.D., Triggiani, A.I., Franciotti, R., Frisoni, G.B., Bonanni, L., De Pandis, M.F., 2017b. Abnormalities of Cortical Neural Synchronization Mechanisms in Subjects with Mild Cognitive Impairment due to Alzheimer's and Parkinson's Diseases: An EEG Study. *J. Alzheimers Dis.* 59 (1), 339–358. <https://doi.org/10.3233/JAD-160883>. PMID: 28621693.
- Babiloni, C., Barry, R.J., Başar, E., Blinowska, K.J., Cichocki, A., Drinkenburg, W.H.I.M., Klimesch, W., Knight, R.T., Lopes da Silva, F., Nunez, P., Oostenveld, R., Jeong, J., Pascual-Marqui, R., Valdes-Sosa, P., Hallett, M., 2020a. International Federation of Clinical Neurophysiology (IFCN) - EEG research workgroup: Recommendations on the frequency and topographic analysis of resting state EEG rhythms. Part 1: Applications in clinical research studies. *Clin. Neurophysiol.* 131 (1), 285–307. <https://doi.org/10.1016/j.clinph.2019.06.234>. Epub 2019 Sep 19. PMID: 31501011.
- Babiloni, C., Blinowska, K., Bonanni, L., Cichocki, A., De Haan, W., Del Percio, C., Dubois, B., Escudero, J., Fernández, A., Frisoni, G., Güntekin, B., Hajos, M., Hampel, H., Ifeachor, E., Kilborn, K., Kumar, S., Johnsen, K., Johannsson, M., Jeong, J., LeBeau, F., Lizio, R., Lopes da Silva, F., Maestú, F., McGeown, W.J., McKeith, I., Moretti, D.V., Nobili, F., Olichney, J., Onofri, M., Palop, J.J., Rowan, M., Stocchi, F., Struzik, Z.M., Tanila, H., Teipel, S., Taylor, J.P., Weiergräber, M., Yener, G., Young-Pearse, T., Drinkenburg, W.H., Randall, F., 2020b. What electrophysiology tells us about Alzheimer's disease: a window into the synchronization and connectivity of brain neurons. *Neurobiol. Aging* 85, 58–73. <https://doi.org/10.1016/j.neurobiolaging.2019.09.008>. Epub 2019 Sep 19. PMID: 31739167.
- Babiloni, C., Arakaki, X., Azami, H., Bennys, K., Blinowska, K., Bonanni, L., Bujan, A., Carrillo, M.C., Cichocki, A., de Frutos-Lucas, J., Del Percio, C., Dubois, B., Edelmayer, R., Egan, G., Epelbaum, S., Escudero, J., Evans, A., Farina, F., Fargo, K., Fernández, A., Ferri, R., Frisoni, G., Hampel, H., Harrington, M.G., Jelic, V., Jeong, J., Jiang, Y., Kaminski, M., Kavcic, V., Kilborn, K., Kumar, S., Lam, A., Lim, L., Lizio, R., Lopez, D., Lopez, S., Lucey, B., Maestú, F., McGeown, W.J., McKeith, I., Moretti, D.V., Nobili, F., Noce, G., Olichney, J., Onofri, M., Osorio, R., Parra-Rodriguez, M., Rajji, T., Ritter, P., Soricelli, A., Stocchi, F., Tarnanas, I., Taylor, J.P., Teipel, S., Tucci, F., Valdes-Sosa, M., Valdes-Sosa, P., Weiergräber, M., Yener, G., Güntekin, B., 2021a. Measures of resting state EEG rhythms for clinical trials in Alzheimer's disease: Recommendations of an expert panel. *Alzheimer's Dement* 17 (9), 1528–1553. <https://doi.org/10.1002/alz.12311>. Epub 2021 Apr 15. PMID: 33860614; PMCID: PMC8647863.
- Babiloni, C., Ferri, R., Noce, G., Lizio, R., Lopez, S., Lorenzo, I., Tucci, F., Soricelli, A., Nobili, F., Arnaldi, D., Famà, F., Orzi, F., Buttini, C., Giubilei, F., Cipollini, V., Marizzoni, M., Güntekin, B., Aktürk, T., Hanoğlu, L., Yener, G., Özbek, Y., Stocchi, F., Vacca, L., Frisoni, G.B., Del Percio, C., 2021b. Resting state alpha electroencephalographic rhythms are differentially related to activity in cognitively unimpaired seniors and patients with alzheimer's disease and amnesic mild cognitive impairment. *J. Alzheimers Dis.* 82 (3), 1085–1114. <https://doi.org/10.3233/JAD-201271>. PMID: 34151788.
- Babiloni, C., Lorenzo, I., Lizio, R., Lopez, S., Tucci, F., Ferri, R., Soricelli, A., Nobili, F., Arnaldi, D., Famà, F., Buttini, C., Giubilei, F., Cipollini, V., Onofri, M., Stocchi, F., Vacca, L., Fuhr, P., Gschwandtner, U., Ransmayr, G., Aarsland, D., Parnetti, L., Marizzoni, M., D'Antonio, F., De Lena, C., Güntekin, B., Yildirim, E., Hanoğlu, L., Yener, G., Gündüz, D.H., Taylor, J.P., Schumacher, J., McKeith, I., Frisoni, G.B., De Pandis, M.F., Bonanni, L., Percio, C.D., Noce, G., 2022. Reactivity of posterior cortical electroencephalographic alpha rhythms during eyes opening in cognitively intact older adults and patients with dementia due to Alzheimer's and Lewy body diseases. *Neurobiol. Aging* 115, 88–108. <https://doi.org/10.1016/j.neurobiolaging.2022.04.001>. Epub 2022 Apr 9. PMID: 35512497.
- Barry, R.J., De Blasio, F.M., Fogarty, J.S., Clarke, A.R., 2020. Natural alpha frequency components in resting EEG and their relation to arousal. *Clin. Neurophysiol.* 131 (1), 205–212. <https://doi.org/10.1016/j.clinph.2019.10.018>. Epub 2019 Nov 20. PMID: 31812081.
- Başar, E., 2012. A review of alpha activity in integrative brain function: fundamental physiology, sensory coding, cognition and pathology. *Int. J. Psychophysiol.* 86 (1), 1–24. <https://doi.org/10.1016/j.ijpsycho.2012.07.002>. Epub 2012 Jul 20. PMID: 22820267.
- Berger, H., 1929. Über das Elektrenkephalogramm des Menschen. *Arch. Psychiat. Nervenkr.* 87, 527–570.
- Brown, L.M., Schinka, J.A., 2005. Development and initial validation of a 15-item informant version of the Geriatric Depression Scale. *Int. J. Geriatr. Psychiatry* 20 (10), 911–918. <https://doi.org/10.1002/gps.1375>. PMID: 16163741.
- Brueggen, K., Fiala, C., Berger, C., Ochmann, S., Babiloni, C., Teipel, S.J., 2017. Early changes in alpha band power and DMN BOLD activity in Alzheimer's disease: a simultaneous resting state EEG-fMRI study. *Front. Aging Neurosci.* 9, 319. <https://doi.org/10.3389/fnagi.2017.00319>. PMID: 29056904; PMCID: PMC5635054.
- Cecchetti, G., Agosta, F., Basaia, S., Cividini, C., Corsi, M., Santangelo, R., Caso, F., Minicucci, F., Magnani, G., Filippi, M., 2021. Resting-state electroencephalographic biomarkers of Alzheimer's disease. *Neuroimage Clin.* 31, 102711. <https://doi.org/10.1016/j.nicl.2021.102711>. Epub 2021 May 29. PMID: 34098525; PMCID: PMC8185302.
- Clayton, M.S., Yeung, N., Cohen Kadosh, R., 2018. The many characters of visual alpha oscillations. *Eur. J. Neurosci.* 48 (7), 2498–2508. <https://doi.org/10.1111/ejn.13747>. Epub 2017 Nov 6. PMID: 29044823.
- Coben, L.A., Danziger, W., Storandt, M., 1985. A longitudinal EEG study of mild senile dementia of Alzheimer type: changes at 1 year and at 2.5 years. *Electro Clin. Neurophysiol.* 61 (2), 101–112. [https://doi.org/10.1016/0013-4694\(85\)91048-x](https://doi.org/10.1016/0013-4694(85)91048-x). PMID: 2410219.
- Colclough, G.L., Brookes, M.J., Smith, S.M., Woolrich, M.W., 2015. A symmetric multivariate leakage correction for MEG connectomes. *Neuroimage* 117, 439–448. <https://doi.org/10.1016/j.neuroimage.2015.03.071>. Epub 2015 Apr 7. PMID: 25862259; PMCID: PMC4528074.
- Crespo-García, M., Atienza, M., Cantero, J.L., 2008. Muscle artifact removal from human sleep EEG by using independent component analysis. *Ann. Biomed. Eng.* 36 (3), 467–475. <https://doi.org/10.1007/s10439-008-9442-y>. Epub 2008 Jan 29. PMID: 18228142.
- Crunelli, V., David, F., Lőrincz, M.L., Hughes, S.W., 2015. The thalamocortical network as a single slow wave-generating unit. *Curr. Opin. Neurobiol.* 31, 72–80. <https://doi.org/10.1016/j.conb.2014.09.001>. Epub 2014 Sep 16. PMID: 25233254.
- Del Percio, C., Infarinato, F., Marzano, N., Iacoboni, M., Aschieri, P., Lizio, R., Soricelli, A., Limatola, C., Rossini, P.M., Babiloni, C., 2011. Reactivity of alpha rhythms to eyes opening is lower in athletes than non-athletes: a high-resolution EEG study. *Int. J. Psychophysiol.* 82 (3), 240–247. <https://doi.org/10.1016/j.ijpsycho.2011.09.005>. Epub 2011 Sep 22. PMID: 21945479.
- Del Percio, C., Derambure, P., Noce, G., Lizio, R., Barrés-Faz, D., Blin, O., Payoux, P., Deplanque, D., Mélégné, D., Chauveau, N., Bourriez, J.L., Casse-Perrot, C., Lanteaume, L., Thalame, C., Dukart, J., Ferri, R., Pascarelli, M.T., Richardson, J.C., Bordet, R., Babiloni, C., 2019. PharmaCog Consortium. Sleep deprivation and Modafinil affect cortical sources of resting state electroencephalographic rhythms in healthy young adults. *Clin. Neurophysiol.* 130 (9), 1488–1498. <https://doi.org/10.1016/j.clinph.2019.06.007>. Epub 2019 Jul 1. PMID: 31295717.
- Delorme, A., Makeig, S., 2004. EEGLAB: an open source toolbox for analysis of single-trial EEG dynamics including independent component analysis. *J. Neurosci. Methods* 134 (1), 9–21. <https://doi.org/10.1016/j.jneumeth.2003.10.009>. PMID: 15102499.
- Duan, W., Chen, X., Wang, Y.J., Zhao, W., Yuan, H., Lei, X., 2021. Reproducibility of power spectrum, functional connectivity and network construction in resting-state EEG. *J. Neurosci. Methods* 348, 108985. <https://doi.org/10.1016/j.jneumeth.2020.108985>. Epub 2020 Oct 24. PMID: 33164816.

- Ebert, U., Kirch, W., 1998. Scopolamine model of dementia: electroencephalogram findings and cognitive performance. *Eur. J. Clin. Invest* 28 (11), 944–949. <https://doi.org/10.1046/j.1365-2362.1998.00393.x>. PMID: 9824440.
- Folstein, M.F., Folstein, S.E., McHugh, P.R., 1975. "Mini-mental state". A practical method for grading the cognitive state of patients for the clinician. *J. Psychiatr. Res* 12 (3), 189–198. [https://doi.org/10.1016/0022-3956\(75\)90026-6](https://doi.org/10.1016/0022-3956(75)90026-6). PMID: 1202204.
- Freedman, M., Leach, L., Kaplan, E., Shulman, K., Delis, D.C., 1994. Clock drawing: a neuropsychological analysis. Oxford University Press, USA.
- Gloor, P., 1994. Berger lecture. Is Berger's dream coming true? *Electro Clin. Neurophysiol.* 90 (4), 253–266. [https://doi.org/10.1016/0013-4694\(94\)90143-0](https://doi.org/10.1016/0013-4694(94)90143-0). PMID: 7512906.
- Gonzalez-Rosa, J.J., Soto-Leon, V., Real, P., Carrasco-Lopez, C., Foffani, G., Strange, B.A., Oliviero, A., 2015. Static magnetic field stimulation over the visual cortex increases alpha oscillations and slows visual search in humans. *J. Neurosci.* 35 (24), 9182–9193. <https://doi.org/10.1523/JNEUROSCI.4232-14.2015>. PMID: 26085640; PMCID: PMC6605156.
- Hughes, S.W., Crunelli, V., 2005. Thalamic mechanisms of EEG alpha rhythms and their pathological implications. *Neuroscientist* 11 (4), 357–372. <https://doi.org/10.1177/1073858405277450>. PMID: 16061522.
- Jack Jr, C.R., Bennett, D.A., Blennow, K., Carrillo, M.C., Dunn, B., Haeblerlein, S.B., Holtzman, D.M., Jagust, W., Jessen, F., Karlawish, J., Liu, E., Molinuevo, J.L., Montine, T., Phelps, C., Rankin, K.P., Rowe, C.C., Scheltens, P., Siemers, E., Snyder, H.M., Sperling, R., 2018. Contributors. NIA-AA Research Framework: Toward a biological definition of Alzheimer's disease. *Alzheimer's Dement* 14 (4), 535–562. <https://doi.org/10.1016/j.jalz.2018.02.018>. PMID: 29653606; PMCID: PMC5958625.
- Jelic, V., Johansson, S.E., Almkvist, O., Shigeta, M., Julin, P., Nordberg, A., Winblad, B., Wahlund, L.O., 2000. Quantitative electroencephalography in mild cognitive impairment: longitudinal changes and possible prediction of Alzheimer's disease. *Neurobiol. Aging* 21 (4), 533–540. [https://doi.org/10.1016/s0197-4580\(00\)00153-6](https://doi.org/10.1016/s0197-4580(00)00153-6). PMID: 10924766.
- Jensen, O., Mazaheri, A., 2010. Shaping functional architecture by oscillatory alpha activity: gating by inhibition. *Front Hum. Neurosci.* 4 (4), 186. <https://doi.org/10.3389/fnhum.2010.00186>. PMID: 21119777; PMCID: PMC2990626.
- Joshi, S., Li, Y., Kalwani, R.M., Gold, J.I., 2016. Relationships between Pupil Diameter and Neuronal Activity in the Locus Coeruleus, Colliculi, and Cingulate Cortex. *Neuron* 89 (1), 221–234. <https://doi.org/10.1016/j.neuron.2015.11.028>. Epub 2015 Dec 17. PMID: 26711118; PMCID: PMC4707070.
- Jovicich, J., Babiloni, C., Ferrari, C., Marizzoni, M., Moretti, D.V., Del Percio, C., Lizio, R., Lopez, S., Galluzzi, S., Albani, B., Cavaliere, L., Minati, L., Didic, M., Fiedler, U., Forloni, G., Hensch, T., Molinuevo, J.L., Bartrés Faz, D., Nobili, F., Orlandi, D., Parnetti, L., Farotti, L., Costa, C., Payoux, P., Rossini, P.M., Marra, C., Schönknecht, P., Soricelli, A., Noce, G., Salvatore, M., Tsolaki, M., Visser, P.J., Richardson, J.C., Wiltfang, J., Bordet, R., Blin, O., Frisoni, G.B., 2019. The PharmaCog Consortium. Two-Year Longitudinal Monitoring of Amnesic Mild Cognitive Impairment Patients with Prodromal Alzheimer's Disease Using Topographical Biomarkers Derived from Functional Magnetic Resonance Imaging and Electroencephalographic Activity. *J. Alzheimers Dis.* 69 (1), 15–35. <https://doi.org/10.3233/JAD-180158>. PMID: 30400088.
- Jung, T.P., Makeig, S., Humphries, C., Lee, T.W., McKeown, M.J., Iragui, V., Sejnowski, T.J., 2000. Removing electroencephalographic artifacts by blind source separation. *Psychophysiology* 37 (2), 163–178. PMID: 10731767.
- Klimesch, W., 1997. EEG-alpha rhythms and memory processes. *Int J. Psychophysiol.* 26 (1–3), 319–340. [https://doi.org/10.1016/s0167-8760\(97\)00773-3](https://doi.org/10.1016/s0167-8760(97)00773-3). PMID: 9203012.
- Klimesch, W., 1999. EEG alpha and theta oscillations reflect cognitive and memory performance: a review and analysis. *Brain Res Brain Res Rev.* 29 (2–3), 169–195. [https://doi.org/10.1016/s0165-0173\(98\)00056-3](https://doi.org/10.1016/s0165-0173(98)00056-3). PMID: 10209231.
- Knaut, P., von Wegner, F., Morzelewski, A., Laufs, H., 2019. EEG-correlated fMRI of human alpha (de-)synchronization. *Clin. Neurophysiol.* 130 (8), 1375–1386. <https://doi.org/10.1016/j.clinph.2019.04.715>. Epub 2019 May 24. PMID: 31220698.
- Kondacs, A., Szabó, M., 1999. Long-term intra-individual variability of the background EEG in normals. *Clin. Neurophysiol.* 110 (10), 1708–1716. [https://doi.org/10.1016/s1388-2457\(99\)00122-4](https://doi.org/10.1016/s1388-2457(99)00122-4). PMID: 10574286.
- Kouzuki, M., Asaina, F., Taniguchi, M., Musha, T., Urakami, K., 2013. The relationship between the diagnosis method of neuronal dysfunction (DIMENSION) and brain pathology in the early stages of Alzheimer's disease. *Psychogeriatrics* 13 (2), 63–70. <https://doi.org/10.1111/j.1479-8301.2012.00431.x>. PMID: 23909962.
- Kramberger, M.G., Kåreholt, I., Andersson, T., Winblad, B., Eriksdotter, M., Jelic, V., 2013. Association between EEG abnormalities and CSF biomarkers in a memory clinic cohort. *Dement Geriatr. Cogn. Disord.* 36 (5–6), 319–328. <https://doi.org/10.1159/000351677>. Epub 2013 Sep 10. PMID: 24022277.
- Laufs, H., Holt, J.L., Elfont, R., Krams, M., Paul, J.S., Krakow, K., Kleinschmidt, A., 2006. Where the BOLD signal goes when alpha EEG leaves. *Neuroimage* 31 (4), 1408–1418. <https://doi.org/10.1016/j.neuroimage.2006.02.002>. Epub 2006 Mar 13. PMID: 16537111.
- Liu, A.K., Dale, A.M., Belliveau, J.W., 2002. Monte Carlo simulation studies of EEG and MEG localization accuracy. *Hum. Brain Mapp.* 16 (1), 47–62. <https://doi.org/10.1002/hbm.10024>. PMID: 11870926; PMCID: PMC6871820.
- Marino, M., Liu, Q., Brem, S., Wenderoth, N., Mantini, D., 2016. Automated detection and labeling of high-density EEG electrodes from structural MR images. *J. Neural Eng.* 13 (5), 056003. <https://doi.org/10.1088/1741-2560/13/5/056003>. Epub 2016 Aug 3. PMID: 27484621.
- Mattsson, N., Andreasson, U., Persson, S., Arai, H., Batish, S.D., Bernardini, S., Bocchio-Chiavetto, L., Blankenstein, M.A., Carrillo, M.C., Chalbot, S., Coart, E., Chiasserini, D., Cutler, N., Dahlfors, G., Duller, S., Fagan, A.M., Forlenza, O., Frisoni, G.B., Galasko, D., Galimberti, D., Hampel, H., Handberg, A., Heneka, M.T., Herskovits, A.Z., Herukka, S.K., Holtzman, D.M., Humpel, C., Hyman, B.T., Iqbal, K., Jucker, M., Kaeser, S.A., Kaiser, E., Kapaki, E., Kidd, D., Klivenyi, P., Knudsen, C.S., Kummer, M.P., Lui, J., Lladó, A., Lewczuk, P., Li, Q.X., Martins, R., Masters, C., McAuliffe, J., Mercken, M., Moghekar, A., Molinuevo, J.L., Montine, T.J., Nowatzke, W., O'Brien, R., Otto, M., Paraskevas, G.P., Parnetti, L., Petersen, R.C., Prvulovic, D., de Reus, H.P., Rissman, R.A., Scarpini, E., Stefani, A., Soininen, H., Schröder, J., Shaw, L.M., Skinningsrud, A., Skrogstad, B., Spreer, A., Talib, L., Teunissen, C., Trojanowski, J.Q., Tumani, H., Umek, R.M., Van Broeck, B., Vanderstichele, H., Vecsei, L., Verbeek, M.M., Windisch, M., Zhang, J., Zetterberg, H., Blennow, K., 2011. The Alzheimer's Association external quality control program for cerebrospinal fluid biomarkers. *Alzheimers Dement* 7 (4), 386–395 e6. doi: 10.1016/j.jalz.2011.05.2243. Erratum in: *Alzheimers Dement* 2011 Sep;7(5):556. PMID: 21784349; PMCID: PMC3710290.
- Morris, J.C., 1993. The Clinical Dementia Rating (CDR): current version and scoring rules. *Neurology* 43 (11), 2412–2414. <https://doi.org/10.1212/wnl.43.11.2412-a>. PMID: 8232972.
- de Munck, J.C., Gonçalves, S.I., Huijboom, L., Kuijer, J.P., Pouwels, P.J., Heethaar, R.M., Lopes da Silva, F.H., 2007. The hemodynamic response of the alpha rhythm: an EEG/fMRI study. *Neuroimage* 35 (3), 1142–1151. <https://doi.org/10.1016/j.neuroimage.2007.01.022>. Epub 2007 Feb 4. PMID: 17336548.
- Näpflin, M., Wildi, M., Sarnthein, J., 2007. Test-retest reliability of resting EEG spectra validates a statistical signature of persons. *Clin. Neurophysiol.* 118 (11), 2519–2524. <https://doi.org/10.1016/j.clinph.2007.07.022>. Epub 2007 Sep 24. PMID: 17892969.
- Novelli, G., Papagno, C., Capitani, E., Laiacona, M., Vallar, G., Cappa, S.F., 1986. Tre test clinici di ricerca e produzione lessicale. Taratura su soggetti normali. *Arch. di Psicol. Neurol. e Psichiatr.* 4 (47), 477–506.
- Olbrich, S., Mulert, C., Karch, S., Trenner, M., Leicht, G., Pogarell, O., Hegerl, U., 2009. EEG-vigilance and BOLD effect during simultaneous EEG/fMRI measurement. *Neuroimage* 45 (2), 319–332. <https://doi.org/10.1016/j.neuroimage.2008.11.014>. Epub 2008 Nov 28. PMID: 19110062.
- Pascual-Marqui, R.D., 2007. Discrete, 3D distributed linear imaging methods of electric neuronal activity. Part I: exact, zero error localization. arXiv:0710.3341 [Math.-ph]. October-17. (<http://arxiv.org/pdf/0710.3341>).
- Peters, J.C., Reithler, J., Graaf, T.A., Schuhmann, T., Goebel, R., Sack, A.T., 2020. Concurrent human TMS-EEG-fMRI enables monitoring of oscillatory brain state-dependent gating of cortico-subcortical network activity. *Commun. Biol.* 3 (1), 40. <https://doi.org/10.1038/s42003-020-0764-0>. PMID: 31969657; PMCID: PMC6976670.
- Pfurtscheller, G., Lopes da Silva, F.H., 1999. Event-related EEG/MEG synchronization and desynchronization: basic principles. *Clin. Neurophysiol.* 110 (11), 1842–1857. [https://doi.org/10.1016/s1388-2457\(99\)00141-8](https://doi.org/10.1016/s1388-2457(99)00141-8). PMID: 10576479.
- Pineda, J.A., 2005. The functional significance of mu rhythms: translating "seeing" and "hearing" into "doing". *Brain Res Brain Res Rev.* 50 (1), 57–68. <https://doi.org/10.1016/j.brainresrev.2005.04.005>. Epub 2005 May 31. PMID: 15925412.
- Reitan, R.M., 1958. Validity of the Trail Making Test as an Indicator of Organic Brain Damage. *Percept. Mot. Skills* 8, 271–276. <https://doi.org/10.2466/pms.1958.8.3.271>.
- Rey, A., 1968. Reattivo della figura complessa. *Organ. Spec.*, Firenze 25–40.
- Rosen, W.G., Terry, R.D., Fuld, P.A., Katzman, R., Peck, A., 1980. Pathological verification of ischemic score in differentiation of dementias. *Ann. Neurol.* 7 (5), 486–488. <https://doi.org/10.1002/ana.410070516>. PMID: 7396427.
- Rosen, W.G., Mohs, R.C., Davis, K.L., 1984. A new rating scale for Alzheimer's disease. *Am. J. Psychiatry* 141 (11), 1356–1364. <https://doi.org/10.1176/ajp.141.11.1356>. PMID: 6496779.
- Rossini, P.M., Di Iorio, R., Vecchio, F., Anfossi, M., Babiloni, C., Bozzali, M., Bruni, A.C., Cappa, S.F., Escudero, J., Fraga, F.J., Giannakopoulos, P., Guntekin, B., Logroscino, G., Marra, C., Miraglia, F., Panza, F., Tecchio, F., Pascual-Leone, A., Dubois, B., 2020. Early diagnosis of Alzheimer's disease: the role of biomarkers including advanced EEG signal analysis. Report from the IFCN-sponsored panel of experts. *Clin. Neurophysiol.* 131 (6), 1287–1310. <https://doi.org/10.1016/j.clinph.2020.03.003>. Epub 2020 Mar 12. PMID: 32302946.
- Salinsky, M.C., Oken, B.S., Morehead, L., 1991. Test-retest reliability in EEG frequency analysis. *Electro Clin. Neurophysiol.* 79 (5), 382–392. [https://doi.org/10.1016/0013-4694\(91\)90203-g](https://doi.org/10.1016/0013-4694(91)90203-g). PMID: 1718711.
- Sharon, O., Fahoum, F., Nir, Y., 2021. Transcutaneous Vagus Nerve Stimulation in Humans Induces Pupil Dilation and Attenuates Alpha Oscillations. *J. Neurosci.* 41 (2), 320–330. <https://doi.org/10.1523/JNEUROSCI.1361-20.2020>. Epub 2020 Nov 19. PMID: 33214317; PMCID: PMC7810665.
- Sloan, E.P., Fenton, G.W., 1993. EEG power spectra and cognitive change in geriatric psychiatry: a longitudinal study. *Electro Clin. Neurophysiol.* 86 (6), 361–367. [https://doi.org/10.1016/0013-4694\(93\)90131-e](https://doi.org/10.1016/0013-4694(93)90131-e). PMID: 7686470.
- Smailovic, U., Koenig, T., Kåreholt, I., Andersson, T., Kramberger, M.G., Winblad, B., Jelic, V., 2018. Quantitative EEG power and synchronization correlate with Alzheimer's disease CSF biomarkers. *Neurobiol. Aging* 63, 88–95. <https://doi.org/10.1016/j.neurobiolaging.2017.11.005>. Epub 2017 Nov 16. Erratum in: *Neurobiol. Aging* 2020 Jul;91:171. PMID: 29245058.
- Soininen, H., Partanen, J., Laulumaa, V., Helkala, E.L., Laakso, M., Riekkinen, P.J., 1989. Longitudinal EEG spectral analysis in early stage of Alzheimer's disease. *Electro Clin. Neurophysiol.* 72 (4), 290–297. [https://doi.org/10.1016/0013-4694\(89\)90064-3](https://doi.org/10.1016/0013-4694(89)90064-3). PMID: 2467794.
- Tait, L., Özkan, A., Szul, M.J., Zhang, J., 2021. A systematic evaluation of source reconstruction of resting MEG of the human brain with a new high-resolution atlas: Performance, precision, and parcellation. *Hum. Brain Mapp.* 42 (14), 4685–4707. <https://doi.org/10.1002/hbm.25578>. Epub 2021 Jul 5. PMID: 34219311; PMCID: PMC8410546.

- Tanaka, H., Hayashi, M., Hori, T., 1996. Statistical features of hypnagogic EEG measured by a new scoring system. *Sleep* 19 (9), 731–738. <https://doi.org/10.1093/sleep/19.9.731>. PMID: 9122561.
- Vogt, F., Klimesch, W., Doppelmayr, M., 1998. High-frequency components in the alpha band and memory performance. *J. Clin. Neurophysiol.* 15 (2), 167–172. <https://doi.org/10.1097/00004691-199803000-00011>. PMID: 9563585.
- Wan, L., Huang, H., Schwab, N., Tanner, J., Rajan, A., Lam, N.B., Zaborszky, L., Li, C.R., Price, C.C., Ding, M., 2019. From eyes-closed to eyes-open: Role of cholinergic projections in EC-to-EO alpha reactivity revealed by combining EEG and MRI. *Hum. Brain Mapp.* 40 (2), 566–577. <https://doi.org/10.1002/hbm.24395>. Epub 2018 Sep 25. PMID: 30251753; PMCID: PMC6338213.
- Wechsler, D., 1987. *WMS-R: Wechsler Memory Scale-Revised: Manual*. Psychological Corporation, San Antonio, TX.